UNIVERSITY OF WEST ATTICA
SCHOOL OF ENGINEERING
DEPARTMENT OF BIOMEDICAL ENGINEERING

Biocatalytic process engineering with the use of 3D printing technology

THEOFILIA KOULOPOULOU
Registration number: 18388084

Supervisor
Evangelia Pantatosaki, Assistant Professor

Athens 2024

The Three-Member Examination Committee

Supervisor

EVANGELIA PANTATOSAKI
Assistant Professor,
Department of Biomedical Engineering,
University of West Attica,
Attiki, Greece

Evangelia Pantatosaki
Digitally signed by Evangelia Pantatosaki
Date: 2024.10.21 11:43:09 +03'00'

(Signature)

SELIN KARA
Prof. Dr. Ing. Habil.,
Institute of Technical Chemistry,
Leibniz University Hannover,
Germany

(Signature)

ELENA GKANTZOU
Postdoctoral Researcher,
Institute of Technical Chemistry,
Leibniz University Hannover,
Germany

(Signature)

DECLARATION BY THE AUTHOR OF THE DIPLOMA THESIS

The signatory Theofilia Koulopoulou of George, with registration number 18388084, student of the Department of Biomedical Engineering, School of Engineering, University of West Attica, I declare responsibly that:
"I am the author of this Diploma Thesis and any help I had for its preparation is fully recognized and referenced. Also, any sources from which I have used data, ideas, or words, whether exact or paraphrased, are listed in their entirety, with full reference to the authors, the publisher, or the journal, including any sources that may have been used by the internet. I also certify that this work has been written exclusively by me and is a product of intellectual property of both myself and the University of West Attica.
Violation of my above academic responsibility is an essential reason for the revocation of my diploma ".

Date
14/10/2024

(Signature)

ABSTRACT

This diploma thesis investigates the integration of 3D printing technology with biocatalysis to develop advanced microfluidic systems for enzyme immobilization and activity assessment. Research and experimental work were conducted at the Institute of Technical Chemistry, Leibniz University Hannover, Germany, in the Biocatalysis and Bioprocessing research group. This study explores the design and construction of microfluidic reactors using cutting-edge 3D printing techniques in order to optimize enzymatic processes. Our goal is to improve the stability and effectiveness of enzyme immobilization by incorporating surface chemistry techniques like glutaraldehyde cross-linking and coatings with polydopamine and polyethyleneimine. The primary objectives include the development of microfluidic systems for selective enzyme immobilization, assessment of biocatalytic performance under continuous flow conditions, and identification of optimal materials and 3D printing methodologies. Utilizing Fused Deposition Modeling and Stereolithography printing technologies in conjunction with enzyme expression and immobilization techniques, precise microfluidic devices are created for effective enzymatic reactions. These prototypes serve as effective screening platforms and can be parallelized to enhance production capacity, which will help with sustainable chemistry and biotechnology applications. As an example of how different 3D printing materials can be used for biotechnological applications like enzyme immobilization, this work emphasizes on how important microfluidic chip-based assays are for effective and quick screening because of their low reagent amounts, affordability, and rapid throughput. In particular, unspecific peroxygenase from *Agrocybe aegerita* (*Aae*UPO) was successfully immobilized on surface functionalized 3D-printed microfluidic chips made of different materials, as confirmed by a model activity assay. This was the first time that 3D-printed microchips were used for *Aae*UPO immobilization, and the enzyme demonstrated high immobilization and activity yields across various materials and geometries, highlighting the potential for development of a universal immobilization approach.

Key words: 3D Printing, Microfluidics, Enzyme immobilization, Flow Biocatalysis

ΠΕΡΙΛΗΨΗ

Στα πλαίσια της παρούσας διπλωματικής εργασίας διερευνάται ο συνδυασμός της τεχνολογίας τρισδιάστατης εκτύπωσης με τη βιοκατάλυση ροής για την ανάπτυξη προηγμένων μικρορευστομηχανικών συστημάτων για την ακινητοποίηση ενζύμων και την αξιολόγηση της δραστικότητάς τους. Η έρευνα και τα πειράματα εκπονήθηκαν στο Ινστιτούτο Τεχνολογικής Χημείας του Πανεπιστημίου Leibniz, στο Αννόβερο της Γερμανίας, στην ερευνητική ομάδα Βιοκατάλυσης και Βιοεπεξεργασίας. Η συγκεκριμένη μελέτη πραγματεύεται τον σχεδιασμό και την κατασκευή μικρορευστονικών αντιδραστήρων με τη χρήση τεχνικών τρισδιάστατης εκτύπωσης για τη βελτιστοποίηση ενζυμικών διεργασιών. Ο τελικός στόχος είναι η βελτίωση της σταθερότητας και της αποτελεσματικότητας της ακινητοποίησης των ενζύμων με την ενσωμάτωση τεχνικών επιφανειακής χημείας για την τροποποίηση επιφανειών, όπως η διασταύρωση με γλουταραλδεΰδη και οι επικαλύψεις με πολυντοπαμίνη και πολυαιθυλενιμίνη. Οι πρωταρχικοί στόχοι περιλαμβάνουν την ανάπτυξη μικρορευστονικών συστημάτων για την επιλεκτική ακινητοποίηση ενζύμων, την αξιολόγηση της βιοκαταλυτικής απόδοσης σε συνθήκες συνεχούς ροής και τον προσδιορισμό των βέλτιστων υλικών και μεθοδολογιών τρισδιάστατης εκτύπωσης. Χρησιμοποιώντας μεθόδους τρισδιάστατης εκτύπωσης, όπως η Μοντελοποίηση Συντηγμένης Εναπόθεσης (Fused Deposition Modeling) και η Στερεολιθογραφία (Stereolithography), σε συνδυασμό με εξελιγμένες τεχνικές έκφρασης και ακινητοποίησης ενζύμων, δημιουργήθηκαν ακριβείς μικρορευστονικές συσκευές με ενζυμική δράση. Αυτά τα πρωτότυπα χρησιμεύουν ως πλατφόρμες ταυτόχρονης εξέτασης πολλαπλών δειγμάτων, ενώ μπορούν να χρησιμοποιηθούν εν παραλλήλω για αυξημένη παραγωγική ικανότητα. Τέτοιου είδους συστήματα συναντώνται σε εφαρμογές βιώσιμης χημείας και βιοτεχνολογίας. Πιο συγκεκριμένα, η παρούσα εργασία αναδεικνύει τον τρόπο με τον οποίο μπορούν να χρησιμοποιηθούν διαφορετικά υλικά τρισδιάστατης εκτύπωσης για βιοτεχνολογικές εφαρμογές όπως η βιοκατάλυση μέσω ακινητοποίησης ενζύμων. Οι βιοκαταλυτικές διεργασίες σε μικρορευστονικά τσιπ παρέχουν τα πλεονεκτήματα του αποτελεσματικού και γρήγορου ελέγχου των χαμηλών ποσοτήτων αντιδραστηρίων, της προσιτής τιμής και της γρήγορης απόδοσης. Στην παρούσα μελέτη, το ένζυμο μη ειδική υπεροξυγενάση του οργανισμού *Agrocybe aegerita* (*Aae*UPO) ακινητοποιήθηκε με επιτυχία στην επιφάνεια λειτουργικών τρισδιάστατων εκτυπωμένων μικροτσίπ από διαφορετικά υλικά. Πραγματοποιήθηκε μια σειρά πειραμάτων λειτουργικότητας και σταθερότητας του ακινητοποιημένου ενζύμου με τη χρήση συστημάτων συνεχούς ροής. Εν κατακλείδι, αυτή ήταν η πρώτη φορά που χρησιμοποιήθηκαν τρισδιάστατα εκτυπωμένα μικροτσίπ για την ακινητοποίηση της *Aae*UPO και το ένζυμο επέδειξε υψηλές αποδόσεις ακινητοποίησης και δραστικότητας σε διάφορα υλικά και γεωμετρίες, αναδεικνύοντας τη δυνατότητα ανάπτυξης μιας ολιστικής προσέγγισης ακινητοποίησης.

Λέξεις-κλειδιά: Τρισδιάστατη εκτύπωση, Μικρορευστολογία, Ακινητοποίηση ενζύμων, Βιοκατάλυση ροής

Graphical Abstract

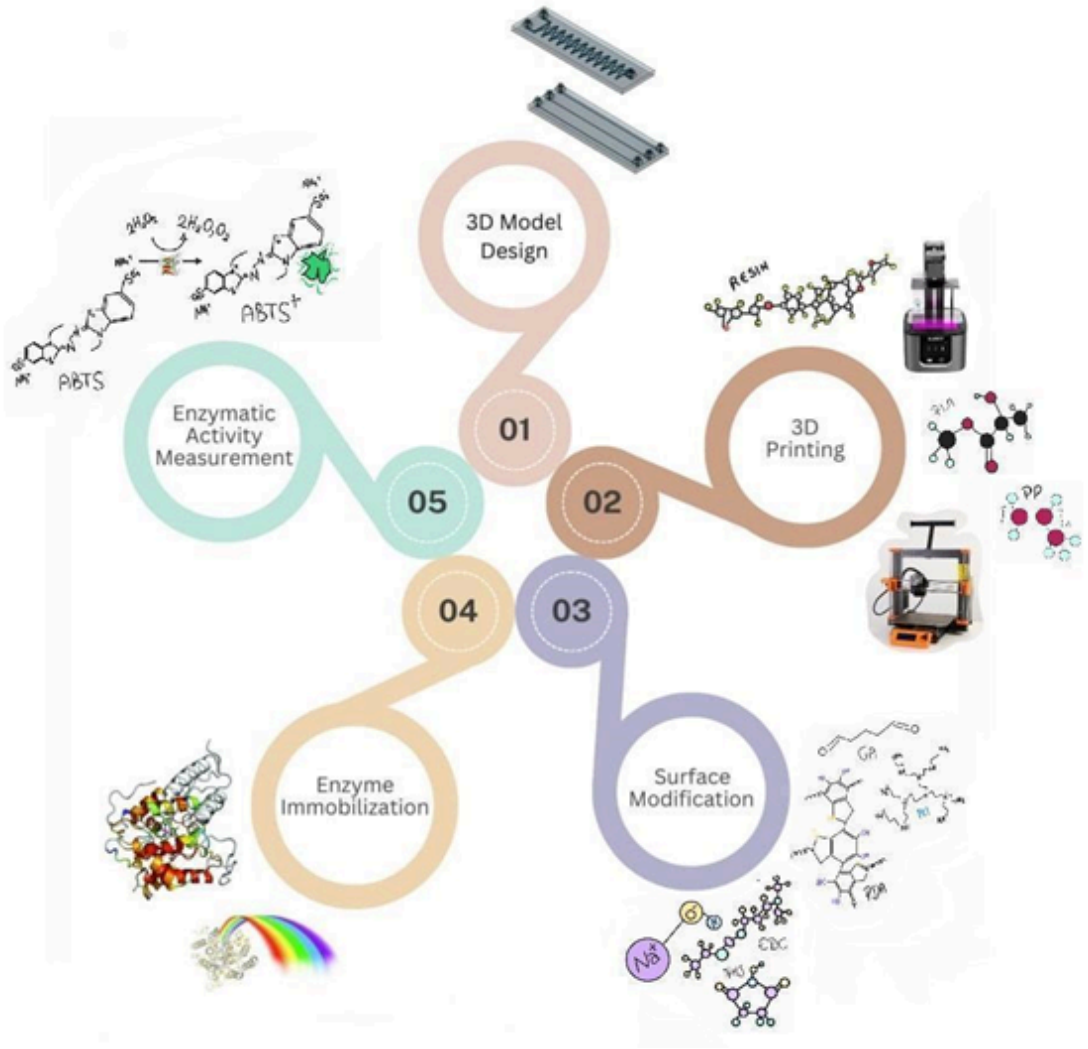

Gratitudes

I wish to convey my heartfelt appreciation to everybody who played a pivotal role in the completion of this diploma thesis.
I would like to express my sincere gratitude to my supervisor and assistant professor, Mrs. Evangelia Pantatosaki, for her invaluable advice and support during my research. Her input was essential to the accomplishment of this endeavor.
I extend my sincere gratitude to Professor and Head of the Institute of Technological Chemistry and the Biocatalysis and Bioprocessing Research Group, Prof. Dr. Ing. Habil. Selin Kara, for her invaluable support and the exceptional opportunity to conduct my diploma thesis experiments in the microfluidics laboratory. Indeed, operating at a facility furnished with instruments and technologies seldom encountered collectively in a single laboratory has significantly enhanced my knowledge and expertise.
I wish to extend my sincere gratitude to my mentor, Dr. Elena Gkantzou, researcher and leader of the microfluidics laboratory team, for her outstanding assistance and unwavering support. Our involvement was essential for enhancing my understanding and effectively concluding the project.
I extend my gratitude to Professor and Chair of my department, Mr. Ioannis Kalatzis, along with all the professors and lecturers in my department, for their unwavering support during my studies and for imparting invaluable information and skills that facilitated my academic growth.
I extend my profound gratitude to my family and friends for their steadfast support, comprehension, trust, and encouragement during this journey. Their presence was indispensable and enabled me to surmount every challenge.

List of Figures

List of Tables

List of Abbreviations

- ABTS: 2,2'-Azino-bis(3-ethylbenzothiazoline-6-sulfonate)
- BCA: Bicinchoninic Acid
- DA: Dopamine
- ddH_2O: Distilled Deionized Water
- EDC: 1-Ethyl-3-[3-dimethylaminopropyl]carbodiimide Hydrochloride
- GA: Glutaraldehyde
- H_2O_2: Hydrogen Peroxide
- KPi: Potassium Phosphate Buffer
- NaOH: Sodium Hydroxide
- PDA: Poly(dopamine)
- PEI: Polyethylenimine
- PLA: Polylactic Acid
- R^2: Coefficient of Determination
- STY: Space-Time Yield

- Sulfo-NHS: N-Hydroxysulfosuccinimide sodium salt
- UPO: Unspecific Peroxygenase
- εABTS: Extinction Coefficient of ABTS (36.8 mM cm^-1)

TABLE OF CONTENTS

1 MOTIVATION AND OBJECTIVES

The biocatalysis sector is progressing rapidly, propelled by the need for more effective and environmentally friendly techniques of chemical synthesis. Unspecific Peroxygenases (UPOs) are versatile biocatalysts enzymes that possess a wide range of substrate specificity and exhibit selective oxidation capabilities [1]. Although UPOs have been characterized as a swiss-army knife in terms of their applicability in oxyfunctionalization chemistry, their stability and efficiency under operational conditions generally limit their applicability [2]. Therefore, it is necessary to develop immobilization techniques and optimize reactor designs in order to improve the performance of UPOs and broaden their industrial applications [3].

Enzyme immobilization and microfluidic system design using traditional methods pose numerous difficulties. Traditional approaches frequently encounter difficulties in achieving accuracy, compatibility with different materials, and the establishment of suitable microenvironments that promote maximum enzyme performance [4]. Consequently, there is an urgent need for biocatalytic systems that are both stable and efficient, capable of operating constantly and in various conditions [5]. The latest progress in 3D printing technology presents encouraging remedies to these constraints. The capacity to construct intricate microfluidic systems with great accuracy and utilize various materials presents fresh opportunities for the advancement of microreactors that will enhance enzyme immobilization and biocatalytic activities [6,7]. Through the utilization of 3D printing, researchers can surpass the limitations of conventional techniques, allowing for the production of personalized microfluidic chips that are specifically intended for biocatalytic applications, such as the sustainable production of pharmacological relevant compounds, CO_2 conversion, bioremediation processes[6,8,9].

This diploma thesis is motivated by the transformative capacity of 3D printing to overcome the constraints of traditional microfluidic and enzyme immobilization technologies. The objective of this research is to utilize 3D printing technology to create microreactor systems that are more efficient and long-lasting, hence improving the catalytic efficiency and stability of UPOs [7].

The main goal of this diploma thesis is to examine and devise techniques for fixing UPOs in microfluidic reactors fabricated by 3D printing technology. This entails the pursuit of multiple crucial objectives:

The initial step involves the development and production of microfluidic devices that are specifically designed for the purpose of immobilizing enzymes [7]. The intention will be achieved by leveraging adequate techniques in 3D printing. This involves the optimization of design parameters and the selection of appropriate materials to guarantee the long-lasting and efficient performance of the microreactors [5,6,8,10.11].

Furthermore, the study prioritizes the improvement of enzyme immobilization techniques by employing innovative surface modification and functionalization approaches. This includes incorporating methods such as polydopamine coating, sodium hydroxide etching, and 1-Ethyl-3-[3-dimethylaminopropyl]carbodiimide

Hydrochloride - N-Hydroxysulfosuccinimide (EDC-NHS) cross-linking to enhance enzyme adhesion and activity [8,11-14].

Another crucial aim is to evaluate the biocatalytic efficiency of the immobilized UPOs in continuous flow operations. The task at hand, entails assessing the effectiveness and reliability of the enzyme systems in different operating settings and improving the designs of the microreactors based on the findings from experiments [5].

Finally, the research seeks to create specific microenvironments within the 3D-printed microfluidic chips that enhance enzyme activity and stability. The objective will be accomplished by investigating various materials and surface chemistry techniques to establish the most favorable conditions for UPO application in continuous flow formats [8].

In summary, this diploma thesis aims to enhance the potential of biocatalytic research by introducing a novel and efficient method for investigating and utilizing enzymes in microreactor systems. The project intends to contribute to the current achievements in biocatalysis and microfluidic technology by attaining these objectives. This will result in the development of creative solutions and advancements for practical and research applications in this sector.

2 THEORETICAL BACKGROUND

2.1 Enzyme Immobilization

Enzyme immobilization on solid supports has become a revolutionary method in the advancement of biocatalysts, providing improved catalytic efficiency under different working conditions [4]. This technique has been acknowledged for its capacity to enhance the thermal, storage, and operational stability of enzymes, augment their resistance against detrimental chemicals, and expand their ability to interact with a wider range of substrates [4]. Enzyme immobilization has the added benefit of simplifying the purification, separation, and recovery of enzymes. This allows for their repeated usage and leads to a large reduction in costs associated with biocatalytic processes [7,15]. Immobilization plays a crucial role in integrating biocatalysts into flow bioreactors, developing multi-enzymatic reaction systems, and addressing effluent disposal problems, all of which are vital for industrial applications [16].

2.2 Flow Biocatalysis

Flow biocatalysis refers to the use of enzymes or other biological catalysts in continuous flow systems to carry out chemical reactions [10,17,18]. It offers notable advantages compared to typical batch procedures in terms of efficiency, scalability, and control over reaction conditions [19,20]. Flow reactors differ from standard batch reactors, because they involve the continuous movement of reactants through the system, as opposed to a static vessel where the reaction occurs. This strategy provides

multiple benefits, such as increased command over reaction parameters, such as temperature, enhanced mass transfer, and the possibility of achieving better levels of productivity in small volumes and reduced amounts of reagents [21]. Flow biocatalysis is highly advantageous in industrial applications that need the efficient expansion of processes. The modular nature of flow reactors facilitates scaling up output by adding more reactors in series or parallel, rather than expanding a single batch reactor. In addition, flow systems exhibit superior heat and mass transfer rates, resulting in a substantial reduction in reaction times, from hours in batch operations to only minutes in flow reactors [17]. This approach is not only more efficient but also adheres to the principles of green chemistry by reducing waste and energy usage [18,22].

2.3 Enzyme immobilization in microfluidic reactors

Enzyme immobilization is a major area of global research, with a focus on developing new techniques and enhancing existing ones due to its significant potential. The development of microfluidic reactors has significantly enhanced the field of enzyme immobilization, offering a highly effective platform for carrying out biocatalytic processes in a regulated and uninterrupted manner [17]. Microfluidic systems are especially suitable for conducting high-throughput screening and parallelized processes, which makes them extremely important in industrial applications that prioritize efficiency and scalability [7]. Incorporating immobilized enzymes into these systems has several advantages, such as improved enzyme durability, the ability to reuse them, and the capability to perform reactions continuously in a flowing manner [10,23]. Implementing these strategies not only enhances the overall efficiency of the biocatalytic processes, but also adheres to the principles of green chemistry by minimizing waste and enhancing the sustainability of the operations [8,18,21].

2.4 Unspecific Peroxygenases (UPOs)

Unspecific peroxygenases (UPOs) are a distinct type of heme-thiolate enzymes that have attracted considerable interest since they can facilitate various oxidative reactions alone by utilizing hydrogen peroxide as the oxidizing agent [27]. Since being discovered by the Ullrich group in 2004, UPOs have shown impressive adaptability in the process of adding oxygen to various substances [27]. This makes them extremely valuable in areas such as bioremediation, synthetic chemistry, and the pharmaceutical industry [24,25].

The identification of UPOs was a notable breakthrough in enzyme technology, namely in the complex domain of C-H bond oxyfunctionalization [26]. The enzyme AaeUPO, derived from the basidiomycete *Agrocybe aegerita*, was initially categorized as a haloperoxidase. However, subsequent research led to its reclassification as an unspecific peroxygenase (EC 1.11.2.1). This new classification acknowledges the enzyme's wide variety of substrates and distinctive catalytic features, as described by Ullrich et al. in 2004 [27]. UPOs possess the ability to specifically oxidize C-H, C=C, and C-C bonds without requiring any cofactors except H_2O_2, which makes them extremely efficient biocatalysts [24,27-31].

The catalytic mechanism of UPOs revolves around the activation of hydrogen peroxide at the heme active site [27]. In this site, the iron core is coordinated by a thiolate ligand derived from a cysteine residue [2]. This reaction produces a very reactive iron-oxo intermediate that helps transfer an oxygen atom to the substrate, allowing various oxidative transformations as hydroxylation, epoxidation, sulfoxidation, and dealkylation [1,2,25,32]. The unusual reactivity and stability of UPOs are based on their structural similarities to cytochrome P450 enzymes and their utilization of H_2O_2 instead of molecular oxygen [29,30,31].

UPOs have become more prevalent in industrial settings because of their versatility and effectiveness in a wide range of operations [24,28]. Within the pharmaceutical sector, it plays a significant role in the manufacturing of active pharmaceutical ingredients (APIs) and the synthesis of intricate natural compounds, by generating (R)-1-phenylethanol [3,17,24]. They are also important in the fragrance industry [33]. Their capacity to selectively oxidize substrates is especially helpful in these processes [25]. Further research focused on enhancing enzyme stability, comprehending reaction processes, and broadening the scope of substrates suitable for UPO-catalyzed reactions will increase their usefulness in industrial biocatalysis [34].

UPO immobilization in flow reactors has been studied before using a packed-bed reactor approach, which was proved ideal for large-scale production, offering high efficiency [3]. However, rapid prototyping and high-precision applications created the need of exploring reactors with compact dimensions (microfluidic reactors) to accurately manipulate reaction parameters, providing an optimal setting for enzyme-catalyzed reactions [10,11]. Microfluidic devices not only enable quick screening but also improve the scalability of biocatalytic processes, hence increasing their efficiency and sustainability [6,7,23,35]. By incorporating UPOs into these systems, their exceptional catalytic effectiveness and long-term stability can be utilized for continuous flow reactions, which are crucial for sustainable industrial processes. The integration of UPO into microfluidic devices hasn't been yet explored, making this the first official study about it, a notable progress in the realm of biocatalysis [7].

2.5 3D Printing and Flow Biocatalysis

Three-dimensional (3D) printing, or additive manufacturing, has transformed the fabrication of intricate structures by allowing the step-by-step creation of products directly from digital models [36]. This method has been extensively utilized in diverse domains, such as biocatalysis, for the purpose of fabricating tailored microfluidic devices to immobilize enzymes and facilitate reactions based on fluid flow [3,6]. 3D printing is a useful tool in the construction of improved bioreactors because it allows for the design and creation of complex microenvironments that are customized for certain biocatalytic processes [14].

By incorporating 3D-printed microfluidic devices into flow biocatalysis, it becomes possible to accurately manipulate fluid dynamics, temperature gradients, and substrate concentrations [37]. These factors play a crucial role in enhancing enzyme efficiency. 3D printing aids in the quick creation of prototypes and allows for iterative design

enhancements, which in turn supports the ongoing development of microfluidic systems for biocatalytic applications [36].

The integration of 3D printing and flow biocatalysis signifies a notable advancement in the research of creating sustainable and effective biocatalytic procedures [6,37]. These technologies have the potential to greatly transform the manufacturing of medicines, fine chemicals, and other valuable goods by allowing for exact control and optimization of reaction conditions [5,17].

2.5.1 Fused Deposition Modeling (FDM)

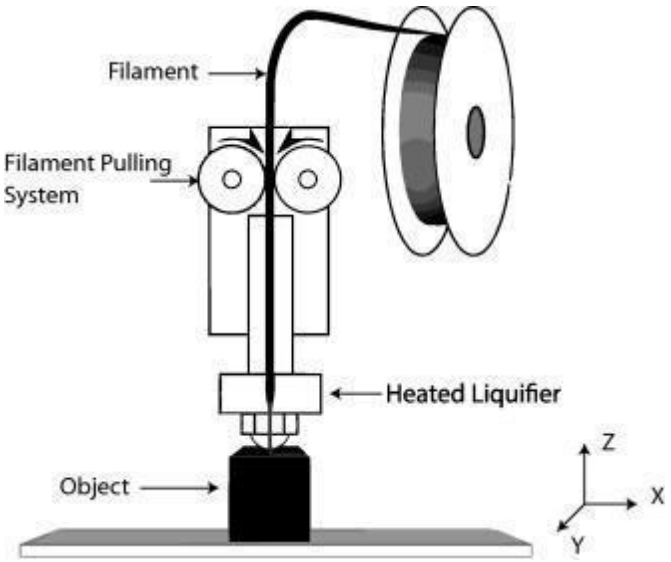

Figure 1. Fused Deposition Modeling Technique adopted from [38].

Fused Deposition Modeling (FDM), commonly known also as fused filament fabrication (FFF), is a widely used additive manufacturing process that is recognized for its user-friendly nature and adaptability [36]. Thermoplastic filaments in FDM are heated and pushed through a nozzle, causing them to melt. They are then deposited layer by layer in a precise manner based on computer designs. This method can handle a wide range of materials, such as polylactic acid (PLA), Polypropylene (PP), Acrylonitrile Butadiene Styrene (ABS), Polyethylene terephthalate glycol-modified (PETG), and others [39]. As a result, it is appropriate for various applications, including quick prototyping, customized manufacturing, and the creation of functional end-use parts and complex geometries [40].

The fundamental mechanism of FDM is centered on precise stepper motors, which control the motion of the nozzle based on G-code instructions produced by a slicing software. The procedure commences by introducing thermoplastic filament into the printer, where it undergoes heating and is subsequently extruded through the nozzle. As the filament travels through the heated nozzle, it undergoes a process of melting and becomes a semi-liquid substance [38]. The temperature is carefully regulated to manage its viscosity and how it flows. The material is methodically and carefully placed layer by layer onto a build platform or on top of previous layers, following a predetermined pattern obtained from a CAD model that has been divided into separate layers. The platform undergoes progressive movements to accommodate each layer.

After being deposited, the liquid substance rapidly cools and hardens, forming a smooth and continuous link with the layers that were previously laid down. The systematic process of depositing layers one by one guarantees the structural strength and precise dimensions of the printed object [41].

Scientific research has greatly enhanced the comprehension and utilization of FDM technology in multiple important fields of study [37,42]. The field of material science is dedicated to improving the mechanical characteristics, thermal stability, and biocompatibility of filament materials. Ongoing research is investigating the usage of new materials such as carbon fibers and metal-infused filaments to expand the range of possible applications [43,44]. The scientific literature extensively discusses process optimization, focusing on parameters such as nozzle temperature, print speed, layer thickness, and infill density. The goal is to decrease flaws and enhance mechanical strength and surface smoothness. Thorough mechanical characterization entails subjecting printed parts to various types of stress in order to evaluate factors like tensile strength, impact resistance, and fatigue behavior. This process ensures that the parts work reliably in a wide range of applications. The capabilities of FDM in biomedical engineering have revolutionized medical practice by facilitating the creation of anatomical models, surgical guidance, and prosthesis that are tailored to individual patients. Ongoing scientific research is dedicated to improving the compatibility of printed medical devices with living tissues and optimizing sterilizing techniques to meet strict healthcare regulations [37,42].

Polylactic acid (PLA) is a biodegradable thermoplastic polymer that is created by polymerization of lactic acid, which is obtained by the fermentation of renewable resources like corn starch or sugarcane. PLA is highly researched for its ability to interact well with living tissues and break down naturally over time, making it well-suited for use in packaging, biomedical devices, and additive manufacturing (3D printing) [45]. The polymer demonstrates a comparatively low glass transition temperature and mild mechanical characteristics, with its deterioration predominantly taking place under industrial composting settings. Although PLA has a reduced carbon footprint than plastics made from petroleum, its environmental effects depend on how well it is processed at the end of its lifecycle. PLA is frequently modified to change certain properties, such as its ability to attract water, the amount of energy required to change its surface, the presence of reactive groups, and its level of roughness. These adjustments are essential for improving the material's performance and increasing its suitability in many fields [45,46]. Widely used since years, PLA is a delegate filament with improved characteristics for 3D pritning without requiring any post-processing after printing.

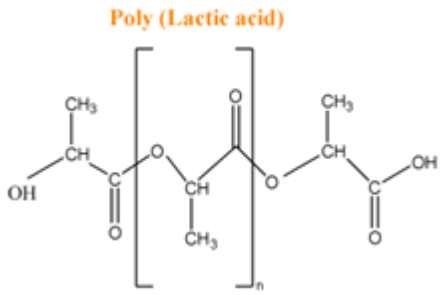

Figure 2. Chemical structure of Polylactic Acid (PLA) generated in ChemDraw.

Polypropylene (PP) is a thermoplastic polymer created by combining propylene monomers, which are hydrocarbons obtained from the refining of petroleum. It is distinguished by its exceptional chemical resistance, robust mechanical strength, and enduring thermal stability, which contribute to its extensive global usage as one of the most prevalent plastics [38]. Polypropylene (PP) is employed in a wide array of applications, encompassing packaging, automotive components, textiles, and medical equipment. The toughness and resistance to fatigue of the material are attributed to its semi-crystalline structure, while its lightweight qualities are a result of its low density. Although of the marvelous properties of polypropylene, such as its remarkable chemical resistance, in bibliography there are only few examples of applications. This is occurring because of its peculiarty in 3D printing, as it is extremely difficult to find the optimum adjustments and achieve a flawless print. Raised temperatures in contribution with layer adhesion and warping have been some of the obstacles why polypropylene is not a preferable material for the users.

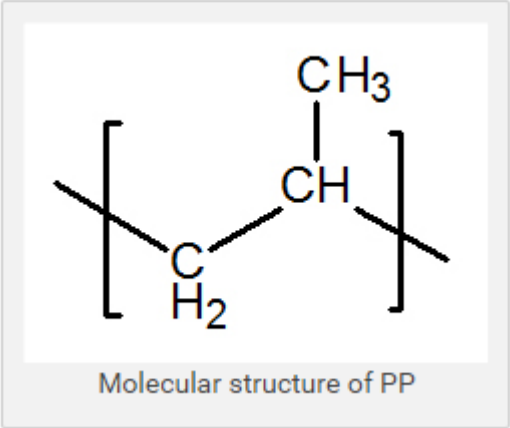

Figure 3. Chemical structure of Polypropylene (PP) adopted from [47].

2.5.2 Resin 3D Printing

2.5.2.1 Stereolithography (SLA)

Stereolithography (SLA) is a venerable and widely recognized light-based 3D printing method. The process utilizes a photopolymerization technology, wherein a UV laser is employed to solidify a liquid resin layer, in a layer by layer fashion [36]. The laser is used to solidify the resin and create a three-dimensional object by tracing the cross-section of each layer. The SLA process is renowned for its remarkable accuracy and ability to produce complex shapes with impeccable surface finishes [40]. However, due to its utilization of point-by-point laser scanning, the printing process typically requires more time and may incur increased costs.

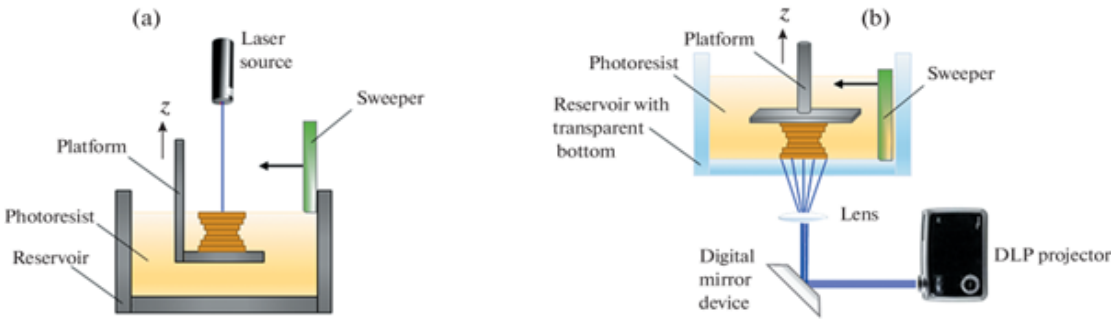

Figure 4. Schematic representation of SLA (a) and DLP (b) devices adopted from [48].

2.5.2.2 Digital Light Processing (DLP)

Digital Light Processing (DLP) is again a light-based 3D printing technique that uses a digital micromirror device (DMD) to project an entire layer's image onto the resin simultaneously, resulting in a faster printing process [36,49]. In comparison to SLA, this technique has a higher printing speed as it solidifies the entire layer simultaneously rather than using a laser to trace it. DLP is widely recognized for its excellent precision and resolution, allowing for precise manipulation of the curing process and achieving immaculate surface finishes [46,48]. It is commonly used in situations that require accurate and high-quality outputs [42].

2.5.2.3 Masked Stereolithography (MSLA)

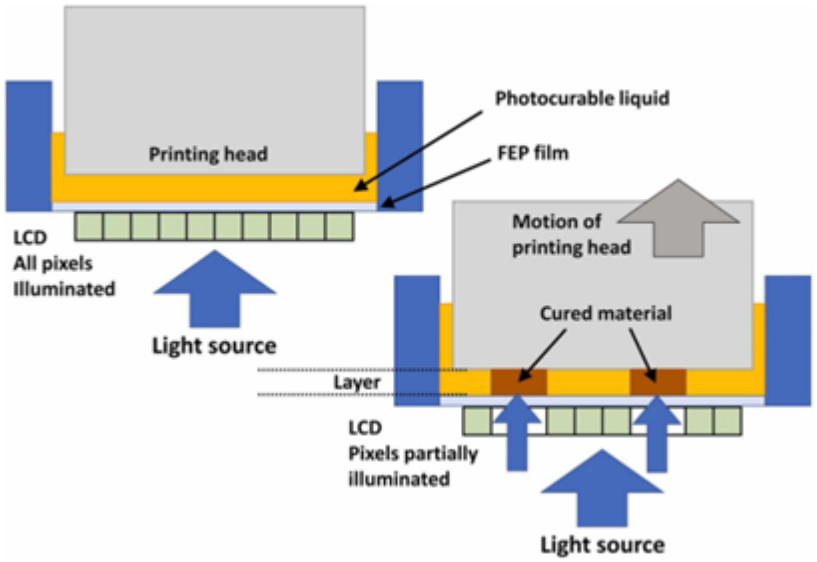

Figure 5. Schematic representation of MSLA device adopted from [50].

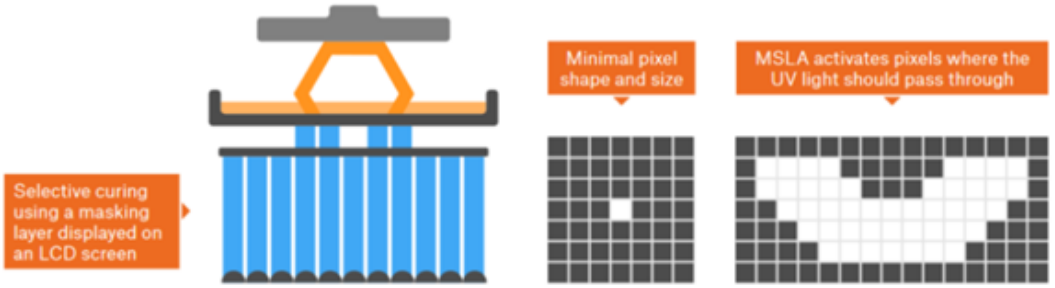

Figure 6. Schematic illustration of Masked Stereolithograohy technology adopted from [49].

Masked Stereolithography (MSLA) is also a light-based 3D printing technology that utilizes an LCD screen to project the image of each layer onto the resin, hence enhancing the possibilities of conventional SLA. Like DLP, this technology also cures the entire layer simultaneously, significantly accelerating the printing process compared to SLA. MSLA combines the rapid layer curing of DLP with the superior resolution and accuracy of SLA, offering a cost-effective and efficient solution for various applications. The MSLA technology utilizes an LCD mask that offers a variety of design options and may be used with a wide range of materials.

Masked Stereolithography (MSLA) is a resin-based 3D printing technique that involves using photopolymer resins that are cured by a UV light source with the help of a digital mask [51]. It utilizes UV LED lights, which generate UV radiation in the region of 385-405 nm, as the main light source for curing photopolymer resin. The selection of this specific wavelength has a direct impact on both the rate at which polymerization occurs and the ultimate mechanical characteristics of the printed products. The printer utilizes an LCD screen instead of a laser to selectively block UV light, thereby displaying each layer of the 3D model that has been cut from a CAD file [50]. The LCD screen's transparent regions allow UV light to solidify resin beneath it, creating a pattern that matches the current slice. This process guarantees accurate production of intricate shapes with a high level of detail, as stated in references [52].

The printer's resin tank is filled with liquid photopolymer resin, which is then dispensed onto the build platform as part of the printing process. The composition, viscosity, and curing behavior of the resin have a substantial influence on both the print quality and mechanical qualities of the final product. Manufacturers frequently provide specialized resins tailored for their printers to attain the correct mechanical strength, surface finish, and post-processing needs. During the printing process, the build platform gradually moves downwards (or the resin tank moves above) as each layer is solidified, which helps in creating layers efficiently and improving the overall speed and productivity of the printer. After the printing process, objects are subjected to solvent cleaning to eliminate any remaining uncured resin. Subsequently, they undergo final curing under UV light to assure full polymerization and enhance their mechanical properties [38].

Photopolymer resin is a liquid substance made up of oligomers, monomers, and photoinitiators [53]. It undergoes a photochemical reaction when it is subjected to ultraviolet (UV) or visible light. Exposing the resin to this factor initiates the process

of polymerization, causing it to transform into a firm and inflexible state. The primary application of this technology is in stereolithography (SLA), masked stereolithography (MSLA) and digital light processing (DLP) 3D printing. It allows for the accurate creation of intricate shapes and high-resolution structures [54]. The resin's capacity to attain intricate surface finishes is a result of its regulated curing process. Nevertheless, the composition frequently contains chemical additions that may give rise to environmental and health concerns.

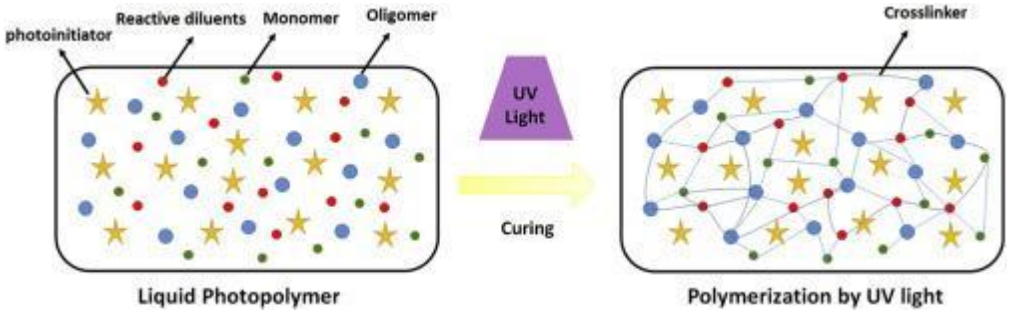

Figure 7. Principal schematic of the photopolymerization process adopted from [53].

Photopolymer plant-based resin is an environmentally-friendly alternative to conventional photopolymer resins. It is made from renewable, bio-based materials like soy or maize and it is water-washable, meaning that organic solvents for post-processing after printing can be avoided. This resin is designed to undergo curing and solidification when exposed to ultraviolet (UV) or visible light, much as standard photopolymer resins [55].

2.6 Advances in biocatalytic process engineering

2.6.1 Recent advancements in Unspecific Peroxygenases (UPOs) for Biocatalysis

Unspecific Peroxygenases (UPOs) have become prominent in biocatalysis because of their capacity to carry out selective oxidations, which is particularly important in pharmaceutical production [28]. Current developments are centered on improving the stability and expanding the spectrum of substrates that can be used by UPOs [1,28]. Recent studies have shown notable enhancements in the catalytic efficiency and stability of UPOs by optimizing the reaction conditions, making them more suitable for industrial applications like the manufacturing of (R)-1-phenylethanol, a crucial intermediate in fragrance and pharmaceutical synthesis [3,56].

2.6.2 Microfluidic systems for enhanced biocatalysis

The study of fluid flow dynamics and channel layout has garnered significant interest in the development of microfluidic chips for enzyme immobilization and enhanced reaction efficiency [17,19]. In general, microreactors (below 1mm internal diameter) have shown improved flow, lower pressure drops, good temperature transfer and

efficient mixing in comparison with traditional reactors that are more complicated and also require bigger quantities, making the first more suitable for research studies regarding sustainable biocatalysis [10]. To prolong the duration of contact between substrates and mounted enzymes, narrower tubes are employed to regulate the flow of fluid [57,58].

Recent advancements in microfluidic technology have introduced novel designs that target the enhancement of mixing efficiency, particularly under low Reynolds number settings [59]. A significant progress has been made in the development of a two-layer serpentine chaotic micromixer, which greatly enhances the efficiency of mixing in different flow conditions. This design is highly effective for applications that require thorough and fast mixing. It surpasses previous mixer designs in terms of performance, as evidenced by simulations and experiments conducted by S. Hossain and colleagues [60]. The goal is to maintain the enzymes' integrity by obtaining high efficiency in biocatalytic processes, even at low Reynolds numbers.

2.6.3 Surface modification techniques

The employment of surface modification techniques, such as the coating of materials with polydopamine (PDA), has been thoroughly studied in order to improve the characteristics of materials used in biochemical applications [12]. The integration of PDA in various materials has demonstrated enhanced surface properties, facilitating the attachment and growth of cells [13]. This technique has also demonstrated efficacy in the production of microfluidic chips using 3D printing and the immobilization of enzymes [7].

The application of sodium hydroxide (NaOH) as a surface coating is a well-established method in the sectors of biochemistry and medicine. The hydrophilicity of the surface is enhanced and its reactivity for further functionalization activities is increased through the addition of hydroxyl groups during the NaOH treatment [8,11]. This alteration is essential for enhancing the process of biomolecule adsorption, promoting cell adhesion, and improving the overall compatibility with living organisms, especially in biosensing platforms and biomedical equipment [61].

2.6.4 Bioconjugation Techniques

Polyethylenimine (PEI) is renowned for its abundant reactive amino groups. It plays a crucial role in enhancing the surface chemistry of enzyme immobilization by creating a protective milieu. This microenvironment significantly enhances the stability and loading capacity of immobilized biomolecules [13,62]. The combination of PEI and Polydopamine (PDA) results in a synergistic coating that combines the cationic reactivity of PEI with the adhesive strength of PDA [63,64]. This coating offers several reactive sites for further chemical alterations. This mixed coating not only enhances surface properties and promotes enhanced cell adhesion and proliferation, but also forms a durable and enduring layer that is vital for tissue engineering and regenerative medicine purposes. The combination of PEI and PDA provides enhanced

stability and versatility for various biological applications, representing a significant advancement in surface modification [14].

The use of 1-Ethyl-3-[3-dimethylaminopropyl]carbodiimide hydrochloride (EDC) and N-hydroxysuccinimide (NHS) together has become a widely accepted method for connecting molecules with amino groups in biochemical assays and medicinal research [16]. This technique is highly advantageous for chemically bonding biomolecules, peptides, or polymers together, since it facilitates the formation of stable amide bonds between carboxyl groups and primary amines [1,65].

Glutaraldehyde (GA) has long been an important substance in the field of enzyme immobilization, particularly for activating surfaces that have been treated with polydopamine (PDA) and include amino groups [12,66]. Robust and consistent covalent immobilization is crucial for maintaining enzyme activity and stability in various applications, and it is significantly enhanced when GA is employed to activate these aminated groups [16]. GA is commonly employed as a cross-linking agent due to its heterofunctional characteristics [11]. By utilizing Schiff base chemistry, it is possible to establish strong linkages between surfaces and biomolecules [67].

2.6.5 3D Printing for Microfluidics

The progress made in 3D printing technologies, namely in stereolithography (SLA) and fused deposition modeling (FDM), has had a substantial influence on microfluidics [10,37,57]. FDM is an extrusion based tecnique that is depositing a therrmoplastic material and building layer by layer the object on the build platform. SLA, on the contrary, uses a liquid photopolymer resin that is cured by a UV light source and the layers are built up as the object is submerged in the resin. The precision of SLA has facilitated the advancement of intricate microfluidic devices with improved functioning [40]. SLA printing enables the production of complex and precise microfluidic channels, which play a critical role in enhancing fluid dynamics in biocatalytic applications [52,58]. However, polylactic acid prints with the use of FDM technology have shown remarkable results for biocompatibility and sustainable applications [6,8].

3 MATERIALS AND METHODS

3.1 Materials and Equipment

Enzymes

- *Aae*UPO supplied from Aminoverse S.A (The Netherlands)

Substrates

- ABTS supplied from TCI Chemicals

Solvents

- H2O highly clean double distilled
- Methanol supplied from FischerScientific
- Ethanol supplied from FischerScientific
- Isopropanol supplied from FischerScientific
- H_2O_2 35% supplied from Merck

Buffers

- buffer Citrate phosphate, 100 mM pH 4.4M
- buffer Sodium phosphate, 50 mM, pH 7
- buffer Tris/HCl 50 mM, pH 8.5
- buffer KPi 50 mM, pH 7.4

Other Reagents

- N-Hydroxysulfosuccinimide sodium salt (Sulfo-NHS) supplied from Merck
- N-(3-Dimethylaminopropyl)-N-ethylcarbodiimide hydrochloride (EDC-HCl) supplied from Merck
- Polyethyleneimine, Branched, M.W. 600, 99%, Liquid supplied from ThermoFischer Scientific
- Glutaraldehyde, concentration: 25% solution supplied from ThermoFischer Scientific
- Dopamine Hydrochloride, supplied from Sigma-Aldrich
- PierceTM BCA Protein Assay Kit supplied from ThermoFischer Scientific

Equipment and Supplies

- NE-1200 Twelve-Channel Programmable Syringe Pump supplied from Darwin Microfluidics
- Multiskan Sky Photospectrometer supplied from ThermoFischer Scientific
- Syringes 1 mL Omnifix-F supplied from B. Braun
- Blunt-End Luer Lock Syringe Needles supplied from Darwin Microfluidics
- Tygon Tubing, diameter of 1.5 mm supplied from Darwin Microfluidics
- Parafilm supplied from Carl Roth

3D Printing Materials and Equipment

- PLA Filament Crystal Clear, diameter of 1.75 mm supplied from Filamentum
- PP Filament Clear Natural, diameter of 1.75 mm supplied from Verbatim Europe
- Plant Based Clear Resin supplied from Anycubic
- 3D FDM Printer Original Prusa i3 MKS3+ supplied from PRUSA Research
- 3D MSLA Printer Elegoo Mars 4 Ultra supplied from Elegoo Official

3.2 Methods

3.2.1 Three-Dimensional Design

The microfluidic chips were intricately designed using the Fusion 360 CAD program developed by Autodesk (California, USA). This program facilitated accurate modeling and customisation of the chip geometries, guaranteeing that the complex channels and reservoirs were optimized for fluid dynamics and compliance with the FDM and MSLA printing processes.

3.2.1.1 Single flow reactor

The microfluidic chip has dimensions of 23 mm x 75 mm, with a thickness of 3 mm. The channels have a length of 70 mm and an internal diameter of 0.75 mm (unless stated otherwise). The chip includes inlets and outlets that have an internal diameter of 1.5 mm and a height of 4.8 mm.

The designed microfluidic chip served as a highly effective screening platform for biocatalytic applications in a small-scale environment [7]. The design facilitates regulation of fluid flow, enabling the most favorable interaction between enzymes and substrates. The controlled microenvironment guarantees improved catalytic efficiency, making it suitable for uninterrupted biocatalytic activities [5,17]. By harnessing the complex microstructures of the chip, we may enhance the mixing and speed of chemical reactions, so making substantial progress in enzyme-based applications at a reduced size.

3.2.1.2 Mixing reactor

Furthermore, a mixing reactor was developed to meet the demand for enhanced mixing and substrate dispersion. Both of these aspects are essential for the successful catalytic reactions. In terms of its external dimensions, this reactor is identical to the single-flow reactors. It has a chip size of 23 millimeters by 75 millimeters and a thickness of three millimeters. Having said that, it possesses an interior structure that is more complicated. In the mixing reactor, the main channel is 0.75 millimeters diameter wide, which is comparable to the width of the single-flow reactor. However, the mixing reactor also includes diagonal channels that are 0.30 millimeters wide. This design incorporates eleven mixing units while the final capacity is 80 microliters.

3.2.2 Slicing

3.2.2.1 FDM Slicing

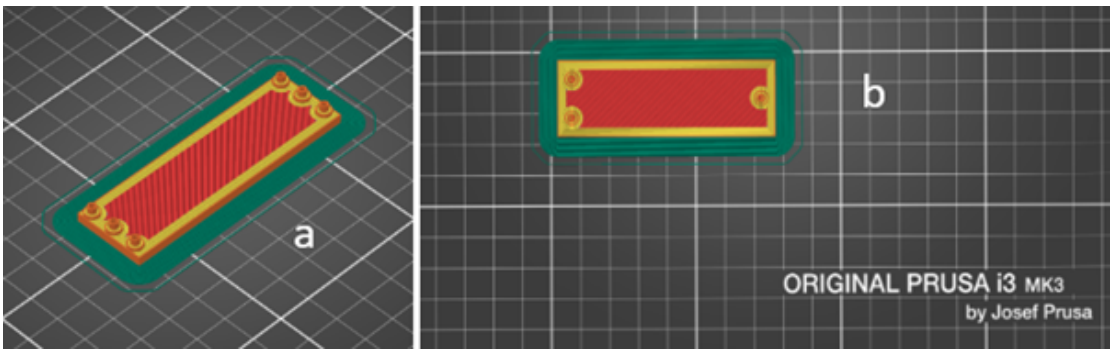

Figure 8. View of model as it appears on the slicing software Prusa Slicer. Printing position and orientation on the build plate. a)single flow reactor b)mixing reactor.

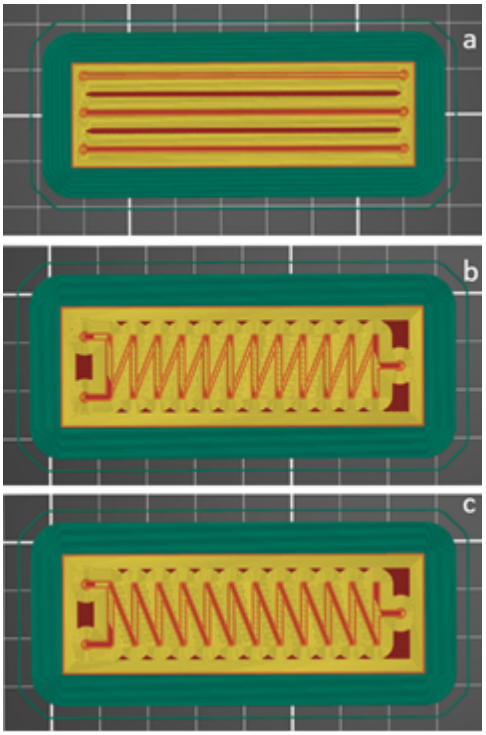

Figure 9. View of models infill in the slicing software Prusa Slicer. a)single flow reactor b)mixing reactor down side c)mixing reactor upper side.

The software utilized for FDM printing was PrusaSlicer. All printing parameters were optimized regarding the necessities of every design and taking into account the printer's errors. The parameters specified in Table 1 consisted of a layer height of 0.07 mm to provide high resolution and fine detail and a minimum of seven perimeters to guarantee the structural integrity. A 100% infill was utilized to optimize the robustness and longevity of the printed components. The brim width was adjusted to 7 mm without any gap in order to improve the adhesion of the bed. The print speeds were carefully adjusted: perimeters, small perimeters, and exterior perimeters were printed at a speed of 10 mm/s, travel moves at a speed of 130 mm/s, and the first layer at a speed of 20 mm/s. The print speed was adjusted to be slower for the first layers in order to achieve better adhesion on the build surface. For the rest of the print the speed was set to be faster to reduce print time but slow enough to ensure precise control over the printing process and good adhesion between layers. The diameter of the extruder nozzle was 0.4 mm, which is commonly chosen because it provides a balance between detail and speed and is compatible with a wide range of filaments.

The nozzle temperature is material-specific and ensures that the filament melts and flows properly. The Crystal Clear PLA filament (Fillamentum, 1.75mm) was printed with a nozzle temperature of 215 °C for the first layer and 210 °C for successive layers. The bed temperature was maintained at a constant 60 °C to enhance adhesion and prevent warping.

On the other hand, the Polypropylene Verbatim Filament (Clear Natural, 1.75 mm) needed adjustments in order to accommodate its specific material qualities, as outlined in Table 1. The nozzle temperature was consistently set at 220 °C for every layer, while the bed temperature was increased to 100 °C in accordance with the manufacturer's guidelines. A polypropylene tape with adhesive properties was used to guarantee the correct bonding of the polypropylene to the build platform. After each print, any stray fibers or residues were carefully removed from the reservoirs to guarantee the purity and accuracy of the following prints. Importantly, no extra materials were used during the FDM process for both materials, showcasing the printer's capacity to effectively manage intricate shapes and protrusions.

3.2.2.2 SLA Slicing

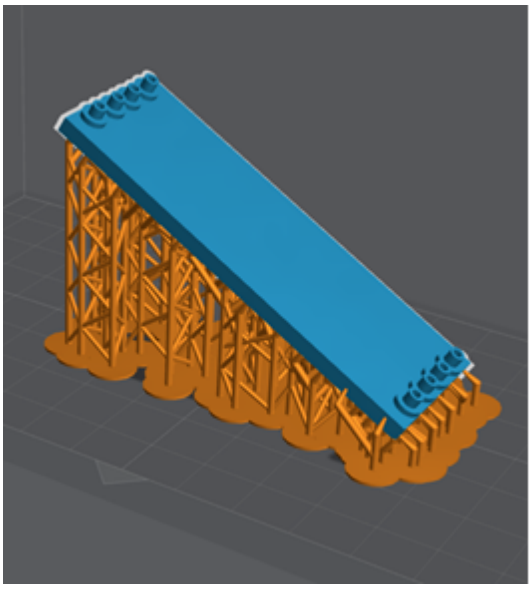

Figure 10. View of model as it appears on the slicing software Lychee Mango. Single flow reactor with 4 channels, orientation 30O and support added.

The SLA printing slicing process was executed using the Lychee Mango Slicer. Table 2 displays the resin configurations for the burn-in layers, which involve a 2.5-second exposure time for four layers, while the transition layers consist of six layers. Initial layers are cured with longer exposure to ensure strong adhesion to the build platform, while four layers help ensure a strong base for the print to adhere to. In the transitional layers the exposure time gradually decreases between the burn-in-layers and normal layers to prevent sudden changes in curing that could lead to defects or uneven layer adhesion. The lift distance was adjusted within the range of 3 mm to 4 mm, while the retract distance was adjusted within the range of 4 mm to 3 mm, in order to prevent layer sticking and ensure smooth transitions without causing damage to the print. The lift speed was set to a range of 60 to 180 mm/min, while the retract

speed was set to a range of 180 to 60 mm/min. Faster speeds can reduce print time, but going too fast can create suction forces that might distort the print. The light intensity was kept at 100% to ensure optimal curing during the exposure time. The standard layers were kept at a thickness of 0.02 mm and exposed for 1.5 seconds. The utilization of these settings, combined with the suitable incorporation of support, guaranteed that the printed structures attained the intended level of resolution and mechanical characteristics.

Table 1. Printing parameters set at the slicing software PrusaSlicer.

FDM	**PLA**	**PP**
Parameter	Value	Value
Layer Height	0.07 mm	0.07 mm
Infill Density	100 %	100 %
Nozzle Temperature	210°C	220°C
Bed Temperature	60°C	100°C
Print Speed	10-40 mm/s	10-40 mm/s
Nozzle Size	0.4 mm	0.4 mm
Filament Diameter	1.75 mm	1.75 mm

Table 2. Printing parameters set at the slicing software Lychee Slicer.

SLA - Resin	
Parameter	Value
Number of Burn In Layers	4
Exposure Time BIL	25 s
Transition Layers Count	6
Layer Thickness	0.02 mm
Exposure Time	1.5 s
Light Intensity	100
Lift and Retract Distance	3 - 4 mm
Lift and Retract Speed	60 - 180 mm/min

Table 1 and Table 2 provide a summary of the printing settings established by the slicing software. The files were saved in a GCODE and GOO type containing the necessary printing instructions for use in the FDM and MSLA 3D printer respectively. The final printed models were devoid of leaks and prepared for subsequent experimentation. A leakage test was performed by injecting the printed models with ddH_2O and allowing them to sit undisturbed for 24 hours at ambient temperature. By the conclusion of this time frame, the overall amount gathered was equal to the overall amount loaded, indicating the absence of any leakage. The leaking test was performed also under flow conditions for different flow rates. Again, the total volumes measured at both the input and outlet of the microreactor were found to be identical.

3.2.3 Printing and Post Processing

During the printing process, we followed a rigorous methodology by employing specialized printers designed for each individual printing technique. We utilized the Prusa i3 MK3+ for FDM printing due of its renowned dependability and accuracy. For MSLA printing, we have selected the Elegoo Mars 4 Ultra due to its well-known reputation for delivering great quality and precision. During the entire procedure, every printer was attentively observed to guarantee optimal performance and swiftly resolve any potential problems. By supervising the process, we were able to implement essential modifications and uphold exceptional levels of excellence, so guaranteeing a triumphant result for every print.

3.2.3.1 Fused Deposition Modeling (FDM) Prints

For FDM-printed models, no post-processing is needed. The printed models are ready to be used and safe to touch. After the printing process is finished, the microreactor was cautiously extracted from the printing bed to prevent any harm. Subsequently, any surplus material such as brims or stringing at the periphery was removed using a specialized cutting tool. This guarantees that the microreactor is prepared for utilization without jeopardizing the structural integrity of its intricate microchannels and characteristics.

3.2.3.2 Masked Stereolithography Apparatus (MSLA) Prints

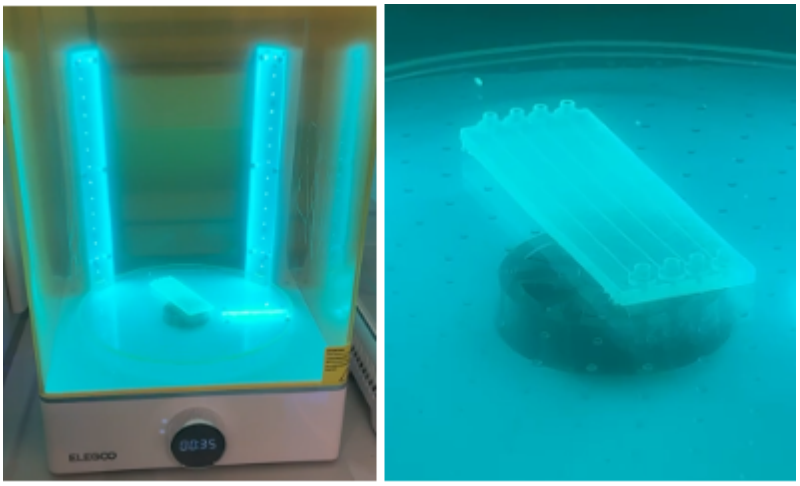

Figure 11. Post processing of resin microreactors.

During handling of SLA printed models, it is essential to guarantee the safety of the user, so protective gloves, glasses and optionally a mask are used. Delicately, the print was detached from the build platform and then cleansed and immersed, utilizing a gentle brush and isopropyl alcohol (IPA) to eliminate any surplus resin [75]. The microchannels were flushed with isopropyl alcohol (IPA) and then any untreated resin was removed by drying them with nitrogen gas (N_2). Carefully, all support structures were removed and the print was submerged in a container of IPA that was delicately stirring and rinsing one more time. Prior to UV light curing, gaseous N_2 was used to

remove untreated resin from the print. Lastly, the construction platform and the working surface were thoroughly cleansed and any contaminated resin was appropriately disposed.

3.2.4 Surface Modification and Enzyme Immobilization in Microfluidic Reactors

Cleaning procedure

The cleaning routine for microfluidic reactors comprises specific procedures designed for PLA, PP, and SLA reactors, which are customized to meet the specific requirements of each material. PLA reactors undergo a two-step cleaning process, starting with a water rinse to facilitate a gentle transition, and then followed by an ethanol rinse. The process entails linking the reactor to a NE-1200 Twelve-Channel Programmable Syringe Pump using Tygon tubing with an inner diameter of 1.5 mm. Additionally, a 1 mL plastic syringe is filled with ddH_2O. The pump is configured to maintain a residence time of 1 minute, which corresponds to a flow rate of 1.499 mL/h for a reactor capacity of 25 μL. Following the water rinse, a 1 mL ethanol rinse is conducted using the same flow rate and residence duration. Subsequently, a drying procedure was performed by purging the reactor with a stream of nitrogen gas for a duration of 60 seconds. For polypropylene (PP) reactors, a rinse with ethanol is conducted. This rinse utilizes the same connection arrangement and flow rate as the polylactic acid (PLA) method. SLA reactors undergo a cleaning process that involves rinsing with water. This method is similar to cleaning PLA reactors, but it excludes the need of ethanol rinse because post-processing with IPA has already been performed. This extensive cleaning procedure guarantees that the reactors are prepped for upcoming tests or applications.

Modification of microchips

3.2.4.1 Case 1: PDA/PEI - GA

Step 1: Application of PDA/PEI coating

The first step of the protocol is to weigh 2mg of dopamine hydrochloride (DA) and 2mg of polyethylenimine (PEI 600) and solubilize with Tris/HCl buffer 50 mM pH 8.5 in a total volume of 1mL (2mg/mL final concentration for both reactants). The PDA/PEI solution is injected into the microchannel through its inlet using a disposable 1mL syringe, until the corresponding reactor volume is filled. DA is oxidized quickly once in contact with buffer, so the filling of the reactors needs to be quick. Subsequently, the reactor is placed in an incubator, at 25°C for a duration of 24 hours. Afterwards, the reactor is subjected to a comprehensive cleaning procedure using ddH2O (at least 10 times the reactors volume) and then dried using N2 gas.

Step 2: Modification of GA Cross-linker

The second step of the protocoI is to prepare a 2.5% GA solution in sodium phosphate buffer 50 mM pH 7. Then, again, a syringe is filled with an amount equal to the

volume of the reactor and the solution is carefully injected [17, 18]. The reactor is covered with parafilm and subjected to incubation at a temperature of 30°C for a duration of 1 hour. Following the cleaning routine, the reactor is cleaned with a volume of ddH2O and dried using N2 gas, as previously mentioned.

Step 3: UPO immobilization process

To immobilize the enzyme, a solution of 1mg/mL UPO is prepared in KPi buffer 50mM pH 7.4. The UPO solution is again inserted into the reactor with the use of a disposal syringe. The reactor is enveloped with parafilm and subjected to incubation at a temperature of 30°C for a duration of 1 hour. Following the incubation period, the enzyme solution is collected and stored at 4°C. Next, the reactor is treated with a cleaning routine with ddH_2O following by drying the reactor using N_2 gas. Subsequently, the microfluidic chips are stored at 4°C until further use.

3.2.4.2 Case 2: NaOH, EDC/NHS

Step 1: Application of NaOH etching

The first step is to prepare a 1M Sodium Hydroxide (NaOH) solution and inject it in the microfluidic channels through the inlets, using a disposable syringe. The microfluidic chips are then incubated for 2 hours at 25°C, as optimized in previous studies [16, 17]. This way, the surface of the material will be enriched with carboxyl and hydroxyl groups that will be used further to perform suitable surface chemistry.

Step 2: Alteration of the EDC-NHS cross-linker

Following the removal of the NaOH solution and cleaning procedure, the reactor is subjected to EDC-NHS crosslinking. A solution is prepared by dissolving 10 mM 1-Ethyl-3-(3-dimethylaminopropyl)carbodiimide (EDC) and 100 mM N-Hydroxysuccinimide-HCl (NHS) in ddH2O and injected though the inlets, using a disposable syringe. An incubation of 1 hour at 25°C follows, after which the solution is removed, and the reactor is cleaned with ddH2O and dried using N2 gas.

Step 3: UPO immobilization process

Afterwards, the reactor is filled with a solution containing UPO at a concentration of 1 mg/mL in KPi buffer with a pH of 7.4. It is then incubated for a duration of 1 hour at 30°C to facilitate the process of enzyme immobilization. Subsequently, the enzyme solution is removed carefully and stored at 4°C. The modified microfluidic chip is rinsed thoroughly with ddH2O and stored at 4°C until further use.

3.2.5 Determination of Free and Immobilized Enzyme Activity

Evaluating the catalytic efficacy of enzymes that are fixed in place provides valuable understanding of how their performance compares to that of enzymes that are not immobilized [68]. This comparison enables an assessment of the possible advantages or disadvantages linked to the immobilization procedure. The activity of an

immobilized enzyme is influenced by two key factors: the accessibility of the substrate to the enzyme's active site and the ease of diffusion for reactants to and from the enzyme. Moreover, the quantity of immobilized enzyme is essential in determining the total activity yield [69].

The peroxidase activity is quantified by monitoring the oxidation of ABTS at room temperature. During this chemical process, ABTS undergoes a conversion into a cation radical known as ABTS+, which is a more stable form [26]. The enzyme's activity is subsequently associated with the concentration of this cation radical, resulting in a noticeable green hue in the solution. The magnitude of this hue, and consequently the enzymatic function, is measured by monitoring alterations in absorbance at 405 nm [3,70].

3.2.5.1 Immobilized Enzyme Activity Measurement

Table 3. Flow rate of enzymatic reaction regarding to the reactors volume and residence time in each case.

3D Printing Technique	Material	Geometry	Reactor Volume (μL)	Residence Time (min)	Flow Rate (mL/h)
SLA	Resin	single flow i.d. 0.5mm	12	2	0.359
SLA	Resin	single flow i.d. 0.75mm	25	2	0.749
FDM	PLA / PP	single flow i.d. 0.75mm	25	2	0.749
FDM	PLA / PP	mixing	80	2	2.399

3.2.5.1.1 Single flow reactor

The enzymatic activity of UPO was evaluated by utilizing the ABTS (2,2'-azino-bis(3-ethylbenzothiazoline-6-sulfonate) as the substrate, following specific conditions. A reaction mixture with a total volume of 250 μL was prepared in a buffer solution with a pH of 4.4, containing citrate phosphate at a concentration of 100 mM. The reaction was conducted at a temperature of 25°C. The reaction mixture comprised 1 millimolar (mM) ABTS, 3 mM H_2O_2.

The total volume of 250 μL was then injected in the microfluidic reactor with a disposable syringe, while maintaining controlled temperature settings. The reaction solution was introduced into the microchannels through Tygon tubing using a Syringe Pump set at a flow rate of 0.749 mL/h, ensuring a controlled and constant flow. The precise flow rate was determined in order to ensure that each aliquot spends exactly 2 minutes in the microfluidic device (residence time). This configuration guarantees a uniform and regulated conversion of the substrate in the enzymatic reaction, allowing for precise evaluation of its activity in a continuous flow.

Following the initiation of the reaction, 25 μL portions of the reaction eluate were collected in a sequential manner into a well plate (full reactor volume processed

equals a reaction cycle). Likewise, the remaining cycles were gathered in separate wells immediately after exiting the tube to ensure that the readings for each cycle were distinct and to confirm their potential for reuse. For each well, 100 μL of reaction buffer was added, resulting in a final volume of 125 μL (a dilution of 1/5), which ensured the best conditions for the assay. Enzymatic activity was determined by performing absorbance measurements in a microplate reader (UV spectrophotometer) at a wavelength of 405 nm. The quantification was done using an extinction coefficient (εABTS) of 36.8 mM cm-1, according to the Beer-Lamberts law.

3.2.5.1.2 Mixing reactor

The mixing reactor facilitates the introduction of ABTS and H_2O_2 through distinct inlets, enabling their combination and thorough mixing within the reactor. The Syringe Pump was adjusted to a flow rate of 2,399 mL/h. This method attains an ultimate concentration of 1 millimolar ABTS and 3 millimolar H_2O_2, guaranteeing the presence of newly generated H_2O_2 to inhibit premature reactions prior to the solution entering the reactor. The mixing process, which is perceptible through the visual transformation of the solution from a bright green hue to a darker green shade after each mixing unit, is intended to optimize the efficiency of the reaction. The combined solution is subsequently gathered at the exit, while each reaction cycle equals 80μL in this case. The reactor's configuration enhances both mixing and reaction regulation. This configuration maximizes the efficiency of enzyme activity by guaranteeing thorough mixing of the reagents and uniform occurrence of the reaction across the microfluidic device.

3.2.5.2 Free Enzyme Activity Measurement

The enzymatic activity was quantified using a spectrophotometric assay under certain circumstances. A reaction mixture with a total volume of 200 μL was made using a citrate phosphate buffer with a pH of 4.4, which had a concentration of 100 mM. The enzyme concentration in the reaction mixture was set to 1 μg/mL. The concentrations of the substrates were kept constant at 1 mM for ABTS and 3 mM for H_2O_2.

The experimental protocol consisted of commencing the chemical reaction and recording the absorbance at a wavelength of 405 nm at 10-second intervals for a total duration of 2 minutes. A blank measurement was also taken to provide a baseline for correction purposes. By employing kinetic monitoring, it became possible to observe in real-time the process of substrate turnover by the enzyme. The buffer conditions were fine-tuned to guarantee the enzyme's stability and activity throughout the assay. Previously acquired kinetic data offered valuable information about the enzymatic activity under these particular experimental conditions, enabling the assessment of the free enzyme's catalytic efficiency.

3.2.6 Estimation of the immobilization yield

3.2.6.1 The Pierce BCA Protein Assay

The Pierce BCA Protein Assay employs reagent A and reagent B, which combine to create a pigmented complex containing proteins that can be measured using spectrophotometry. Reagent A is composed of bicinchoninic acid (BCA) and Cu2+ ions, whereas reagent B is a confidential formulation that improves the colorimetric reaction. The ratio of A to B is essential for the sensitivity of the assay. It is commonly combined at a ratio of 50 parts A to 1 part B, with a total volume of 4,000 μL being prepared. In order to begin the test, 12.5 μL of each sample is mixed with 12.5 μL of distilled water to create a diluted solution. A reference is created by using a blank sample that contains 25 μL of distilled water. Afterwards, 200 μL of the A+B solution is introduced into each well holding the sample or blank, and then incubated at a temperature of 60ºC for a duration of 30 minutes. This is followed by a 5-minute period for the development of color. The measurement of absorbance is performed at a wavelength of 562 nm, allowing for a straightforward determination of protein concentration using a standard curve created with known protein concentrations. The Pierce BCA Protein Assay is highly recognized for its precise measurements and wide range of detection, making it essential in numerous biochemical and biotechnological applications for quantifying proteins [71].

3.2.6.2 Immobilization Yield

Immobilization yield pertains to the efficiency with which biological molecules, such as enzymes or cells, are attached or fastened onto a support material, such as a solid matrix or carrier. The yield plays a critical role in a range of applications, including as biocatalysis, biosensors, and bioseparation, where immobilized biocatalysts or cells frequently demonstrate superior performance compared to their free counterparts. The immobilization yield is determined using a mathematical calculation, which involves dividing the amount of biocatalyst that has been immobilized by the initial amount of biocatalyst utilized, and then multiplying the outcome by 100%. The term "Amount of Biocatalyst Immobilized" refers to the quantity of the biological molecule that has been successfully attached to the support material. On the other hand, the term "Initial Amount of Biocatalyst" refers to the complete quantity of the biological molecule used before immobilization.

An assay was performed on the enzyme solution before and after the immobilization process to measure the quantity of immobilized enzyme. Before loading the enzyme solution into the microreactor, samples were collected. Similarly, after incubation, samples were collected from the corresponding channels and evaluated using the identical technique. The amount of enzyme immobilized in each channel was subsequently determined using Equation (1).

Immobilization yield % = 100 - (enzyme concentration after immobilization) / (enzyme concentration before immobilization) (1)

A high immobilization yield signifies that a substantial portion of the biological molecules have been successfully fixed to the support material. As a consequence, this generally leads to enhanced efficiency and reliability in real-world scenarios. In addition, efficient immobilization minimizes waste and the requirement for excessive

amounts of biological molecules, hence decreasing the overall expenses of the procedure. This is particularly important in large-scale industrial applications where cost-efficiency is crucial. Furthermore, immobilization has the ability to improve the longevity and recyclability of biocatalysts. An elevated immobilization yield guarantees a significant amount of biological molecules for the reaction, potentially enhancing the total activity and lifespan of the biocatalyst [5]. Comprehending and enhancing the immobilization yield is crucial for the advancement of effective biocatalysts and biosensors. This procedure entails the careful selection of suitable support materials and immobilization procedures to optimize the effectiveness of the attachment process [72].

3.2.7 Immobilized Enzyme Activity

Immobilized enzyme activity, measured in units per milligram (U/mg), represents the catalytic efficiency of an enzyme that has been fixed onto a solid support medium. This statistic quantifies the efficiency of the mounted enzyme in converting substrate into product under certain conditions. A single unit (U) of enzyme activity is determined by the quantity of enzyme that facilitates the transformation of one micromole of substrate within a minute, given specific circumstances such as temperature, pH, and substrate concentration. The mathematical calculation for immobilized enzyme activity involves dividing the amount of product generated by the mass of immobilized enzyme and the duration of the reaction as it is shown in the equation (2).

Activity (U/mg) = Amount of Product Formed (P) ÷ [Mass of Imm. Enzyme (E) × Time (T)] (2)

The assessment of enzyme function in its immobilized state relies heavily on the activity of the immobilized enzyme. A high level of activity (U/mg) suggests that the enzyme is efficiently catalyzing activities even while attached to a support. This metric also enables the comparison of various enzyme preparations or immobilization methods, aiding in the selection of the most efficient enzyme-support combination. Gaining insight into the functionality of enzymes while they are in a fixed state helps to enhance the efficiency of reaction conditions and immobilization techniques in order to achieve the highest possible level of productivity. Furthermore, as enzymes frequently display alterations in activity when immobilized as a result of interactions with the support material, assessing activity (U/mg) aids in the evaluation of how immobilization impacts enzyme stability and reusability [17,73].

3.2.8 Activity Yield

Activity yield (%) is a metric employed to evaluate the efficiency of enzyme immobilization by comparing the activity of an immobilized enzyme to its activity in the non-immobilized (free) state. The equation 3 describes the extent to which the enzyme's ability to catalyze reactions is preserved after being immobilized, which serves as an indicator of the effectiveness of the immobilization process. The activity yield (%) is determined mathematically by dividing the activity of the immobilized enzyme (measured in units per milligram) by the activity of the free enzyme

(measured under identical conditions), and then multiplying the quotient by 100% [73].

Activity Yield (%) = Activity of Immobilized Enzyme (U/mg) ÷ Activity of Free Enzyme (U/mg) (3)

Activity yield (%) is a straightforward measure of the amount of enzyme activity that remains after the enzyme is bound to a support material. A high activity yield signifies that the immobilization procedure has successfully maintained the majority of the enzyme's catalytic activity, which is essential for the efficiency of the biocatalyst. This parameter also enables the comparison of various immobilization methods or support materials based on their ability to maintain enzyme activity, facilitating the selection of the most efficient solution for certain applications. Comprehending activity yield is crucial for optimizing immobilization conditions, including pH, temperature, and selection of support material, in order to attain the utmost enzyme activity.

The economic and practical consequences of activity yield are substantial. A high activity yield implies that a less amount of enzyme is required to attain the same level of activity. This can result in cost reduction and enhance the economic feasibility of the process, particularly in industrial settings. Ensuring optimal activity levels of immobilized enzymes is essential in industrial enzyme catalysis to achieve efficient and cost-effective manufacturing processes. In the context of biosensors, it is crucial to achieve a high activity yield in order to preserve the sensitivity and functionality of devices that rely on immobilized enzymes. Ensuring the preservation of high enzyme activity in immobilized forms is crucial in environmental applications, such as bioremediation. This is necessary to effectively degrade contaminants, hence enhancing the efficiency and reliability of the process [73].

3.2.9 Space Time Yield

Space-time yield (STY) is a crucial measure in chemical engineering and reactor design that assesses the efficiency of a reaction process in terms of both space and time. The measurement quantifies the rate at which a product is produced in relation to the size of the reactor and the time it takes for the product to form. STY, or Space-Time Yield, measures the effectiveness of a reactor in converting reactants into products within a certain volume and time. It offers significant information on the productivity and efficiency of the reaction process. Mathematically, the calculation of STY in the Equation (4) involves dividing the yield of the product by the product of the volume of the reactor and the duration of the reaction.

STY = Amount of Product Formed (P) ÷ [Reactor Volume (V) ×Time (T)] (4)

In this context, "product yield" represents the quantity of product produced from the chemical reaction, "reactor volume" indicates the precise area inside the reactor where the reaction takes place, and "time" refers to the duration of the reaction process.

Space-time yield (STY) has extensive applications in diverse areas such as petrochemical processing, medicines, and environmental engineering. It is highly

beneficial for comparing various types of reactors, such as batch and continuous reactors, and for adjusting reaction parameters to attain enhanced productivity [23]. The capability of STY to evaluate and improve the efficiency of reactor operations makes it a crucial instrument in the planning and execution of chemical processes [6].

3.2.10 Stability Studies of the Immobilized UPO

Operational stability pertains to the capacity of an immobilized enzyme system to sustain its catalytic activity across repeated cycles of utilization. This idea is especially crucial in industrial and biotechnological operations, where enzymes are required to operate repeatedly without experiencing a considerable decrease in their activity [15]. Assessing operational stability usually entails monitoring the enzyme's activity during several reaction cycles, and analyzing its ability to consistently convert substrate into product over time.

Operational stability can be evaluated by analyzing the decline in enzyme activity with each subsequent cycle of use, considering the given data and diagram. This decrease in activity can suggest the enzyme's stability under the particular conditions examined. The stability of the 3D printing process can be greatly influenced by various materials and procedures used for immobilization. The choice of materials in 3D printing significantly impacts the immobilization efficiency, substrate interaction, and operational stability of the enzyme. Certain materials can create a more conducive environment for the enzyme, leading to increased operating stability.

Similarly, the technique employed to immobilize the enzyme is vital in determining its long-term stability. Various methods of immobilization, such as covalent bonding, adsorption, or trapping, differ in their ability to maintain the enzyme's structure and function over time. Through the comparison of enzyme activity drop across various combinations of 3D printing materials and immobilization procedures, one can ascertain which combinations provide superior operational stability. For example, if one material exhibits a more gradual decline in activity in comparison to others, it may be better suited for prolonged usage [74].

An important conclusion drawn from this analysis is that by comprehending the patterns in the decrease of enzyme activity, one may determine the ideal combination of 3D printing material and immobilization technology that offers the greatest operational stability. This knowledge is vital for the development of enzyme systems that are efficient and cost-effective, guaranteeing their long-term functionality in many applications.

4 RESULTS AND DISCUSSION

This section outlines a method for designing, 3D printing, modifying, and applying various microreactors as immobilization carriers in the development of advanced biocatalytic systems.

4.1 3D Printed Microreactors

The microreactors were fabricated using three different materials: PLA (Polylactic Acid), PP (Polypropylene), and photopolymer resin, utilizing two different 3D printing technologies: Fused Deposition Modeling (FDM) and Masked Stereolithography (MSLA).

Three distinct types of microreactors were produced: single-flow microreactors with channel diameter of 0.75mm (SINGLE0.75), single-flow reactors with channel diameter of 0.5mm (SINGLE0.5) and mixing reactors (MIXER). For the FDM printing, transparent materials were utilized both for PLA and PP printing. However, due to the inherent nature of this printing process, the printed models do not appear completely transparent, although the microchannels are still visible (Figure 13a). The SLA printing produces models with a greater degree of transparency (Figure 13b), consisting a more advantageous technology for applications that require light-permeable models (e.g. photobiocatalysis). It is also important to note that SLA printing techniques require post-processing, like cleaning and UV treatment, for the model to be ready for further application. In contrast, FDM printing produces ready-to-use and safe-to-touch models.
Cost-effectiveness is another aspect of 3D printing techniques that is taken under consideration, especially for massive production. Different types of printing techniques are characterized regarding a) material consumption and b) material cost. Table 4 presents the different costs related to the models developed in the current diploma thesis. Firstly, it is observed that MSLA technique bears higher costs per model than all the different models produced with FDM technique. In regard to FDM printing of different types of models, it is important to note that the costs are not significantly raised when comparing a 3-channel single-flow microfluidic chip and a micromixer chip. This observation highlights the cost-effectiveness of 3D printing technology as a manufacturing technique for microscale research models.

a) 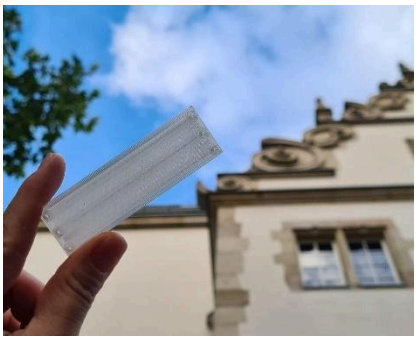 **b)** 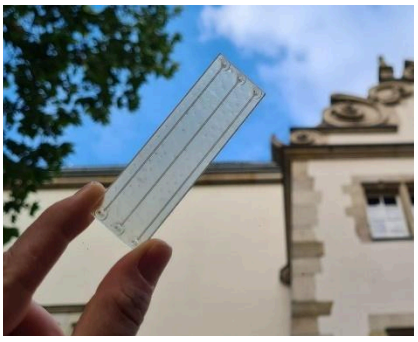

Figure 12. a) PLA model as it appears after printing. b) SLA model as it appears after printing and post processing.

Table 4. Cost-effectiveness of 3 channel-microreactors regarding to the technique and the material used.

Printing Technique	Material	Design	Consumption	Cost (€)
FDM	PLA	single flow	7.13 grams	0.20
FDM	PLA	mixer	7.61 grams	0.21
FDM	PP	single flow	5.12 grams	0.37
FDM	PP	mixer	5.46 grams	0.39
MSLA	Resin	single flow	9.66 mililiters	2.53

4.2 The Design of Microreactors

To improve the efficiency of enzymatic reactions in continuous flow biocatalytic processes carried out within microfluidic systems, the microreactors that were constructed for this study were uniquely tuned to meet specific requirements [37]. Every single design was conscientiously created in order to strike a balance between simplicity, efficiency, and utility, thereby catering to the specific requirements of a variety of catalytic processes. Additionally, the unique interior arrangement of the microreactors allows them to manage larger volumes within a smaller space [23]. This is an essential feature for optimizing operations that involve continuous flow.

4.2.1 Single flow reactors

The first design that was employed in the current diploma thesis is the single-flow microreactor. On a multi-channel microchip, single-flow microreactors were designed with an internal diameter of 0.75 millimeters. When it comes to basic catalytic processes, where simplicity and cost-effectiveness are of the utmost importance, a single flow reactor with straight channels is an excellent option because of its plain design, which makes it much easier to construct. It is also an excellent tool for quick screening of multiple reaction conditions [7]. The microfluidic chip that houses this reactor has dimensions of 23 millimeters by 75 millimeters and a thickness of three millimeters (Figure 13). The channels have a length of 70 millimeters. The inlets and outlets were designed to facilitate the connection with the other parts of the microfluidic system. This particular microreactor has a capacity of 25 microliters, which makes it excellent for reactions that involve a small volume and require precise control over the environment in which the reaction takes place. Because of the ease with which it can be fabricated, this design is advantageous since it lowers production costs and minimizes the possibility of manufacturing errors, ensuring that the performance of the product is uniform throughout all batches [7].

The single-flow microreactor design was also explored in lower internal diameter. Despite the fact that the microfluidic chip's overall dimensions have not changed, the channel diameter was decreased to 0.5 mm, which results in a couple of distinct advantages. Because of the decreased diameter, the surface area-to-volume ratio within the channel is increased, which in turn improves the interaction between the enzyme and the substrate across the channel. When it comes to responses, this change is especially useful for situations in which enhanced surface contact is essential for

enhancing reaction rates or when precise control over fluid dynamics is necessary [52,75]. This particular 0.5 mm channel reactor has a capacity of 12 microliters, making it a more suitable candidate for applications in which the reagents volume is crucial.

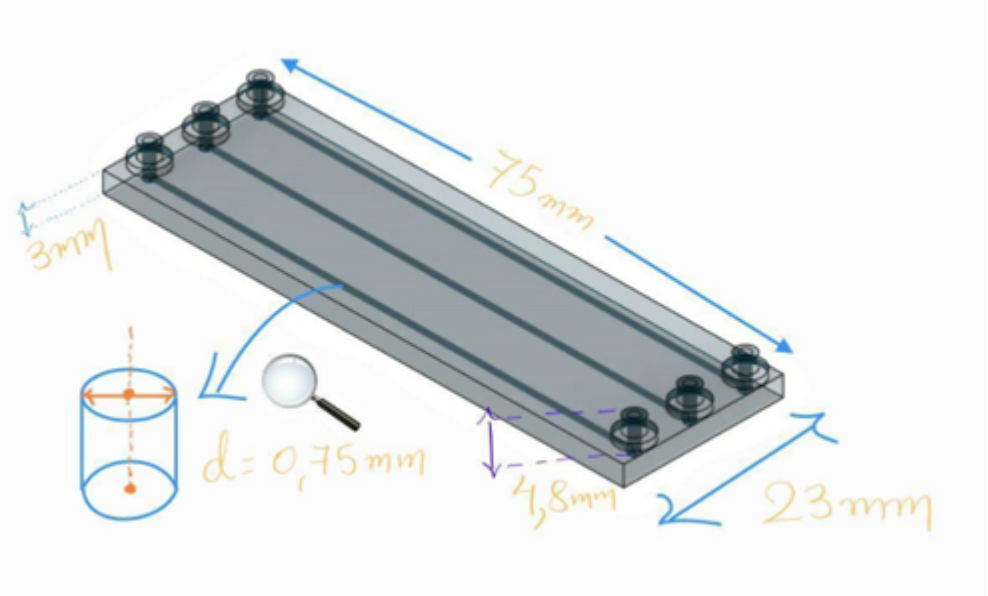

Figure 13. Single flow microreactor model as it appears at the design software.

4.2.2 Mixing reactors

In order to create a microfluidic mixer chip that maximizes the immobilization of enzymes and enhances reaction efficiency, it is crucial to prioritize the study of fluid flow dynamics and the arrangement of channels. The comparison analysis conducted by Anton Enders and his colleagues showed executive results about the mixing performance of the Tesla-like mixer and herringbone (HC) mixer [60]. To optimize fluid flow control and enhance substrate-enzyme interaction, it is necessary to use a more constricted tube that facilitates the passage of substrates through expanded channels. This configuration guarantees enhanced blending and uniform dispersion of the substrate, which are crucial for achieving efficient catalytic reactions. Microfluidic systems generally function at low Reynolds numbers, which prevent turbulent mixing and necessitate the use of diffusive mixing. For effective enzymatic reactions it is also important to limit turbulence and prevent the enzyme from mechanical stress, so maintaining low Reynolds numbers [60]. Nevertheless, in order to mitigate the sluggishness of diffusion, the design of the chip can be enhanced by the utilization of passive mixing methods such as chaotic advection. This entails employing complex channel patterns, such as serpentine or herringbone designs, that augment mixing by elongating and folding the fluid streams, leading to their recombination. These patterns have the possibility to enhance the surface area, facilitating improved interaction between enzymes and substrates, hence enhancing the biocatalytic process.

The mixing microreactor developed in this diploma thesis, was based on the idea given in the publication by S. Hossain and his colleagues [60]. An innovative micromixer with a serpentine design consisting of two layers has been developed to

greatly enhance the efficiency of mixing, especially in situations with low Reynolds numbers. The micromixer reactor utilizes a dual-layer structure with serpentine paths, specifically engineered to improve mixing efficiency when operating at low Reynolds numbers [60]. The layers consist of serpentine patterns that alternate between "inverse N" and "N" shapes in a repetitive sequence. The main channels are positioned perpendicular to the inlets, whereas the connections between fluid flows in the layers occur at the intersections of "X" shapes and vertical segments. Due to the fact that they allow for the constant splitting and rejoining of the fluid streams, these diagonal channels are an essential component of the reactor's mixing capability. In our case, the micromixer design deviates from the references in terms of dimensions (Figure 14). The main channel has a width of 0.75 mm, whilst the diagonal channels have a width of 0.30 mm. This design incorporates eleven mixing units, which makes the reaction mixture substantially more homogenous than it would have been otherwise. The micromixer created has a total capacity of 80μL, accounting for any printing errors, which allows it to accommodate a lot more volume than single-flow reactors and achieves a higher level of mixing efficiency.

The reactor design incorporates several mixing units to ensure uniform catalyst distribution in reactions sensitive to concentration gradients or requiring uniform substrate distribution throughout the reaction chamber. This is especially helpful in reactions that require uniform catalyst distribution. Through the process of repeatedly dividing and rejoining the fluid streams, the mixing reactor reduces the likelihood of different reaction speeds occurring, which ultimately results in an increase in the overall efficiency and dependability of the catalytic process.

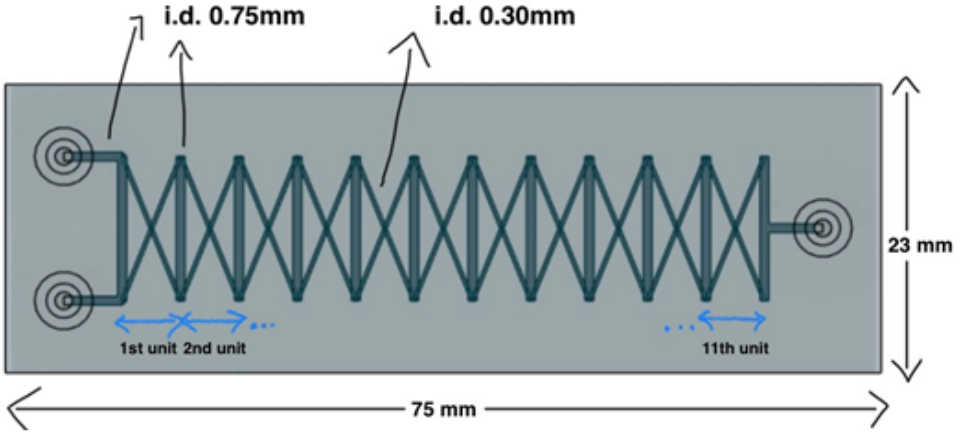

Figure 14. Mixing microreactor model as it appears at the design software.

4.3 Surface Modifications

After exploring the design and printability of the microfluidic reactors, their internal surface was subjected to chemical modification with the aim to render them appropriate carriers for enzyme immobilization. Unspecific peroxygenase (UPO) was used as the model enzyme, and its immobilization was optimized for two different surface modification protocols (PDA based and NaOH based), applied to 3D-printed microreactors made of three different materials (PLA, PP, Resin). ABTS was used as the model substrate for enzymatic activity measurement and its radical cation was quantified with a photometric assay, while H_2O_2 is the main co-substrate used for

UPO activity assays. The concentration of the substrate and co-substrate were optimized with preliminary experiments (data not shown in the current diploma thesis). The reaction conditions were kept identical for each tested system, in order for a comparative analysis of the different protocols and materials to be feasible. The comparative study is analyzed in the following paragraphs and was based on the biochemical characteristics of each obtained system. When it comes to enhancing the performance of microreactors for a variety of biochemical applications, particularly in the context of enzyme immobilization, the findings of this study highlight the significance of individualized surface treatments.

a)

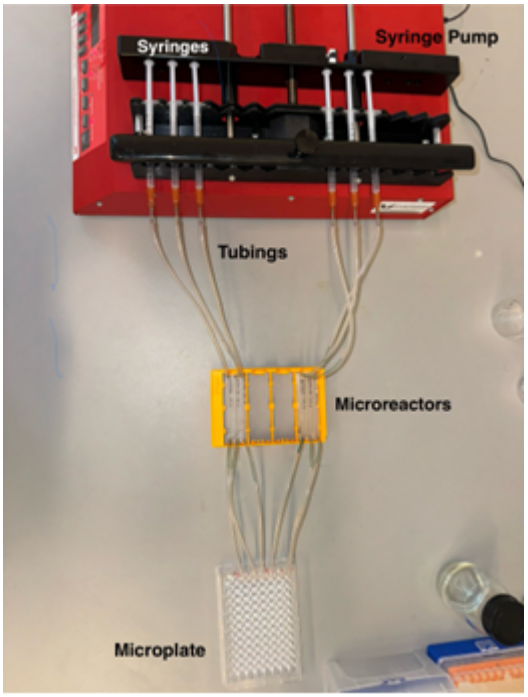

b)

Figure 15. Demonstration of the microfluidic system. a) Syringe Pump, Syringes, Tubings, Microreactors, Microplate, b) Temperature control with a thermistor microdevice designed for microreactors of this size.

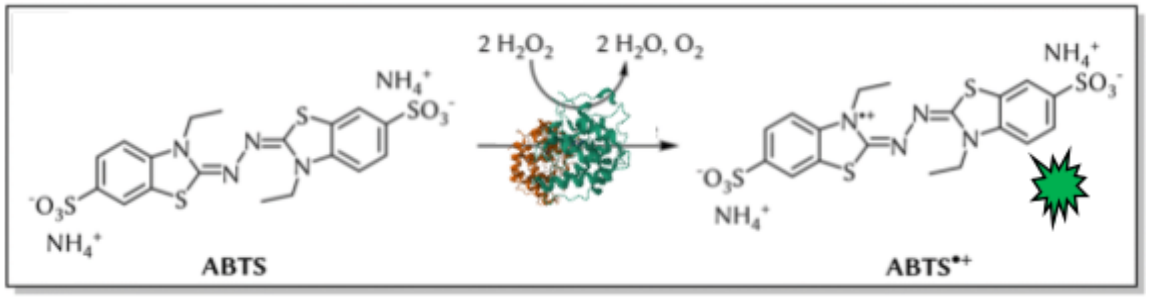

Figure 16. ABTS oxidation and creation of ABTS+ generated in ChemDraw. A green hue is observed when the ABTS is oxidized.

4.3.1 Protocol 1: PDA-based

Surface chemistry techniques play a vital role in enhancing the performance and durability of materials used in biomedical and biotechnological applications. Polydopamine (PDA) is a polymer that is created from dopamine and is inspired by the sticky proteins found in mussels [58]. It forms a strong coating on various surfaces, improving the surface reactivity and allowing for flexible alterations and subsequent bioconjugation.

While PDA can be used for absorptive immobilization of enzymes, without further modifications, the main benefit of covalent immobilization is the increased stiffness of enzymes due to multiple covalent attachments [66]. Using glutaraldehyde to activate the aminated groups in PDA enhances the likelihood of obtaining robust and enduring multipoint covalent immobilization [12]. Enabling undergone reactions with both aldehyde and amine groups, glutaraldehyde possesses dual functionality that is essential for preserving immobilized enzymes, securing the attachment to the scaffolds, especially in processes that need continuous activity [16,77]. This versatile cross-linker establishes strong connections between biomolecules and surfaces via Schiff base chemistry, making it essential for applications that demand stable enzyme immobilization [12,63,78].

Polyethylenimine (PEI) increases surface chemistry by generating a safe milieu for enzymes due to its high density of reactive amino groups [64]. This greatly enhances the loading capacity and stability of immobilized biomolecules by generating a protective microenvironment, hence ensuring their usefulness in diverse biotechnological applications. The combination of PDA and PEI results in a synergistic coating that takes advantage of PDA's strong adhesive properties and PEI's cationic reactivity [12,63]. This coating provides several reactive sites for further chemical modifications [13]. Affirmative, not only improves the surface qualities to facilitate cell adhesion and proliferation, but it also forms a stable and long-lasting layer that is crucial for tissue engineering and regenerative medicine [62].

Regarding to PDA-based surface modification protocol developed in the specific diploma thesis, we employed a dual-layer coating strategy, incorporating a number of reactive groups [63]. The PDA/PEI-GA procedure, as demonstrated in figure 17, is expected to demonstrate considerable enhancements in enzyme binding. By increasing the surface reactivity of the corresponding material and creating an apt environment for the immobilization of enzymes, an improvement in the stability and activity of UPO is ultimately expected.

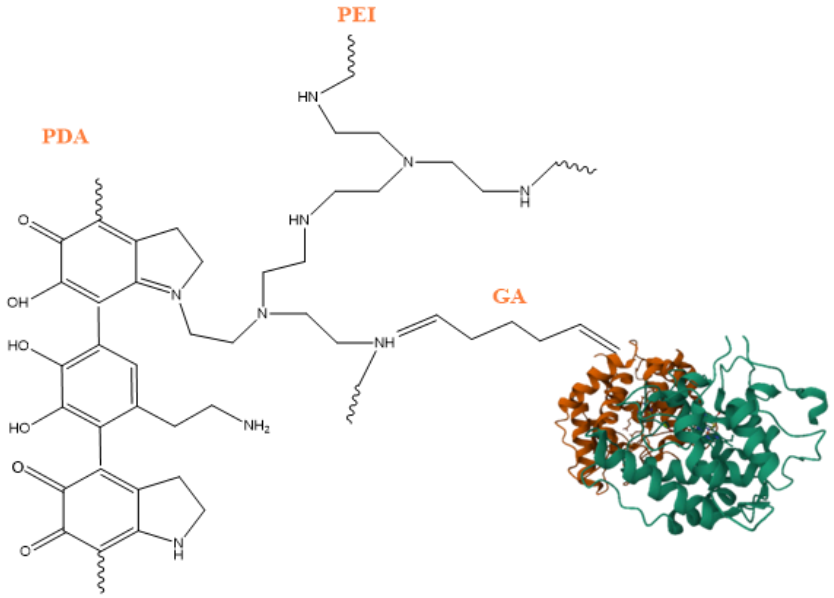

Figure 17. UPO immobilization in case of PDA/PEI - GA adopted from ChemDraw.

In order to accumulate enough proofs for establishing a universal protocol, we investigated several bonding methods, or different scenarios for enzyme immobilization. Elaborating, the surface modification process began each time with the application of polydopamine (PDA) in the microfluidic reactor, which acted as a powerful adhesive layer, whereupon we either omitted some bonds or add more. As an illustration, after the initial application of the PDA layer, we applied glutaraldehyde (GA) to the surface. The capacity of PDA to establish covalent bonds with glutaraldehyde (GA) is very advantageous for producing robust and long-lasting biomolecule connections [65]. In further testing, a modification process that was more complicated was applied to the microreactors, which involved the application of numerous layers of coatings. A layer of polyethyleneimine (PEI) was applied to the surface after the initial PDA coating had been applied. The incorporation of PEI resulted in the provision of extra amino groups, which would promote the formation of more robust chemical interactions during the subsequent GA treatment. The combination of PDA-PEI-GA would result in the creation of a surface that was extremely proper for the attachment of enzymes, which ultimately would lead to an increase in the stability and binding efficiency of UPO. Lastly, a methodology that was even more complicated was applied following consecutive treatment with PDA, GA, and PEI, as well as a second application of GA. The purpose of this intricate modification procedure was to enhance surface hydrophilicity and reactivity by increasing the density of reactive groups and creating more covalent bonds. This would result in an increase in the immobilized enzyme's stability as well as its capacity to bind.

Table 5 demonstrates the results from the application of different scenarios for the PDA-based protocol for the UPO enzyme immobilization in microfluidic reactors. The different scenarios were tested for all three 3D printed materials, with the two different 3D printing techniques. All activity measurements were performed under flow conditions. The values presented are median values from at least 3 different microreactors tested for each specific condition.

Table 5. Biochemical characteristic parameters for UPO immobilized microreactors with PDA-based surface modification protocol. Reaction Conditions: CABTS = 1mM, CH_2O_2 = 3mM, citrate buffer mM pH 4.4, T = 25oC. PDA: polydopamine, PEI: polyethylenimine, GA: glutaraldehyde, E: enzyme.

3D Printing Technique/ Material	Protocol	Immobilization yield (%)	Immobilized enzyme activity (U/mg)	Activty Yield (%)	STY (g/L*h)
FDM - PLA (0,75mm)	PDA/PEI-GA-E	60.09	0.341	27.89	0.990
FDM – PLA (mixer)	PDA/PEI-GA-E	66.03	0.297	77.74	0.863
FDM - PLA (0,75mm)	PDA-GA-E	74.25	0.174	14.21	0.504
FDM - PLA (0,75mm)	PDA-PEI-GA-E	56.47	0.139	11.39	0.405
FDM - PLA (0,75mm)	PDA - GA - PEI - GA -E	34.54	0.239	21.79	0.875
FDM - PP (0,75mm)	PDA/PEI-GA-E	59.22	0.276	20.6	0.802
FDM - PP (mixer)	PDA/PEI-GA-E	60.52	0.255	72.31	0.731
SLA - RESIN (0,75mm)	PDA/PEI-GA-E	54.63	0.161	13.7	0.468
SLA - RESIN (0,5mm)	PDA/PEI-GA-E	55.77	0.324	5.78	0.427
SLA - RESIN (0,75mm)	PDA-GA-E	73.27	0.129	10.54	0.374
SLA - RESIN (0,75mm)	PDA-PEI-GA-E	49.82	0.139	11.37	0.404

Table 5 displays data that compares various surface modification techniques for three types of 3D-printed microreactors, which are constructed using SLA-resin, FDM-PLA and FDM-PP materials when exposed to several surface treatments. The bonding methods tested were PDA/PEI-GA-E, PDA-GA-E, PDA-PEI-GA-E and an extended-chain treatment of PDA-GA-PEI-GA-E. Important metrics for successful immobilization are highlighted. More specifically, we will discuss about immobilization yield (expressed as a percentage), immobilized enzyme activity (measured in U/mg), activity yield (also expressed as a percentage), and space-time yield (STY, measured in g/L*h).

Immobilization yield

The immobilization yield of SLA-Resin treated with PDA-GA-E was 73.27%, indicating its remarkable efficacy in binding enzymes. Nevertheless, when the

treatment becomes more intricate using PDA/PEI-GA-E, the output diminishes to 54.63% and for the PDA-PEI-GA-E even more, to 49.82%. The FDM-PLA microreactors have also a significant immobilization yield of 74.25% when using PDA-GA-E. However, this yield decreases to 60.09% when PEI is included in the PDA/PEI-GA-E treatment. The administration of the combination treatment PDA-GA-PEI-GA-E leads to a substantial decrease to 34.54%, suggesting that the heightened intricacy in surface modification can have an adverse effect on enzyme binding. Highlighted also should be the difference between PDA-PEI-GA and dual-layer PDA/PEI-GA approach, where the first has a yield of 56.47% and the second 60.09%.

Immobilized Enzyme Activity

The enzyme activity of SLA Resin rises as the treatment becomes more pertinent, with a rise from 0.129 U/mg using PDA-GA-E to 0.161 U/mg using PDA/PEI-GA-E. This implies that although the immobilization yield may drop, the functional orientation or accessibility of enzymes improves with more complex treatments. The FDM-PLA exhibits a comparable pattern, wherein the enzyme activity rises from 0.174 U/mg to 0.341 U/mg when subjected to the more complex PDA/PEI-GA-E treatment.

Activity Yield and Space Time Yield

The use of SLA Resin results in a moderate increase in activity yield, rising from 10.54% with PDA-GA-E to 13.7% with PDA/PEI-GA-E. This is accompanied by a comparable rise in STY, from 0.374 g/Lh to 0.468 g/Lh. The FDM-PLA microreactors demonstrate a large improvement in activity yield, reaching 27.89% with PDA/PEI-GA-E, which also results in a notable rise in STY to 0.99 g/L*h. This emphasizes the exceptional catalytic effectiveness of FDM-PLA microreactors, especially when exposed to the PDA/PEI-GA-E treatment.

4.3.2 Protocol 2: NaOH-based

The use of Sodium Hydroxide (NaOH) surface coating is extensively utilized to alter surfaces in diverse biomedical and biochemical applications [11,61]. The use of NaOH increases the hydrophilicity of the surface by eliminating impurities and introducing hydroxyl groups, resulting in a more responsive surface for subsequent functionalization procedures. This technique is crucial for enhancing the surface characteristics that impact the attachment of biomolecules, the adherence of cells, and the general compatibility with living organisms [8].

1-Ethyl-3-[3-dimethylaminopropyl]carbodiimide hydrochloride (EDC) and N-hydroxysuccinimide (NHS) are commonly used in biochemical tests and biomedical research to promote cross-linking reactions involving amines. EDC facilitates the activation of carboxyl groups, leading to the formation of reactive intermediates and NHS is adhering to the stability [16]. These intermediates quickly react with primary amines, resulting in the formation of stable amide bonds. This method is commonly employed to chemically connect biomolecules, peptides, or

polymers, hence improving their durability and effectiveness in biomedical applications such as drug delivery systems and bioconjugation strategies [61,79,80].

In the present diploma thesis, NaOH was utilized to enrich the surface of the material with chemical moieties that would later be activated by the EDC/NHS chemistry as it is shown in figure 18. This way, another covalent immobilization method for the enzyme would be explored.

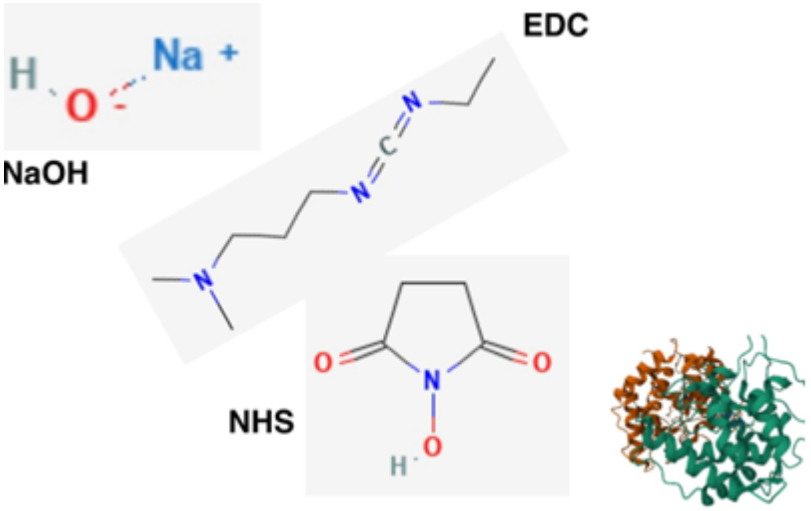

Figure 18. UPO immobilization in case of NaOH - EDC/NHS generated in ChemDraw.

Table 6 demonstrates the results from the application of the NaOH-based surface modification protocol for the UPO enzyme immobilization in microfluidic reactors. The protocol was applied for all three 3D printed materials, with the two different 3D printing techniques. All activity measurements were performed under flow conditions. The values presented are median values from at least 3 different microreactors tested for each specific condition.

Table 6. Biochemical characteristic parameters for UPO immobilized microreactors with NaOH-based surface modification protocol. Reaction Conditions: CABTS = 1mM, CH_2O_2 = 3mM, citrate buffer mM pH 4.4, T = 25oC. NaOH: sodium hydroxide, EDC: 1-Ethyl-3-(3-dimethylaminopropyl)carbodiimide, NHS: N-Hydroxysuccinimide-HCl, E: enzyme.

3D Printing Technique/ Material	Protocol	Immobilization yield (%)	Immobilized enzyme activity (U/mg)	Activty Yield (%)	STY (g/L*h)
FDM - PLA (0,75mm)	NaOH-EDC/NHS-E	45.69	0.174	14.24	0.505
FDM - PP (0,75mm)	NaOH-EDC/NHS-E	34.42	0.157	12.84	0.456
SLA - RESIN (0,75mm)	NaOH-EDC/NHS-E	19.84	0.105	10.81	0.386
SLA - RESIN (0,5mm)	NaOH-EDC/NHS-E	28.59	0.132	8.55	0.304

Table 6 displays the data collected for the evaluation of the three different 3D printing materials after application of the NaOH-EDC/NHS-E approach for optimizing enzyme immobilization in 3D-printed microreactors. Important metrics for successful immobilization are highlighted. More specifically, we will discuss about immobilization yield (expressed as a percentage), immobilized enzyme activity (measured in U/mg), activity yield (also expressed as a percentage), and space-time yield (STY, measured in g/L*h).

Immobilization Yield

The NaOH-EDC/NHS-E treatment for microreactors with a channel of 0.75 mm internal diameter markedly reduces the immobilization yield in comparison with the 0.5 mm (i.d.) channel , reaching 19.84% from 28.59%. That means better enzyme immobilization in smaller channel diameters. The same treatment in FDM-PP microreactors has a most effective immobilization of 34.42% with the FDM-PLA microreactors having again the maximum result of 45.69%.

Immobilized Enzyme Activity

The FDM-PLA microreactors exhibit a maximum enzyme activity of 0.174 U/mg with FDM-PP microreactors following at 0.157 U/mg, while SLA-Resin exhibits less activity with 0.105 U/mg.

Activity Yield and Space Time Yield

The FDM-PLA microreactors have the highest activity yield of 14.24% and an STY of 0.505 g/L*h. Again FDM-PP is following, with the lowest parameters numbers being for SLA-Resin microreactors.

4.4 In-depth Comparative Analysis: Different surface modification protocols

In the previous paragraphs, the results from the application of the two distinct surface modification protocols were presented, for all the different 3D-printing techniques and materials. Herein, a comparative analysis is presented with the most important conclusions regarding the comparison of the applied protocols for the optimum immobilized enzyme efficiency.

The use of PDA/PEI-GA-E protocol in FDM-PLA microreactors results the highest biochemical characteristics with immobilization yield of 60.09%, immobilized enzyme activity of 0.341 U/mg, activity yield of 27.89% and 0.99 g/L*h STY. When applicating the NaOH-EDC/NHS-E protocol the characteristics are significantly reduced for all materials, but still FDM-PLA microreactor is outstanding with the highest results. A remarkable observation could be that SLA-Resin microreactor exhibits slight enhancements in activity yield and STY following NaOH-EDC/NHS-E treatment, but often remains inferior to PDA-treated samples.

The immobilization yield, a critical factor for enzyme binding, serves as an indicator of the efficiency of surface modifications. The use of NaOH-EDC/NHS-UPO treatment leads to lower levels of immobilization and activity yield compared to PDA treatments on all materials. Using NaOH-EDC/NHS treatment on microreactors has a notable decrease also in enzyme activity and space-time yield, resulting in lower rates of product generation. Subsequently, the findings indicate that there is a noticeable decline in the effectiveness of catalysis with NaOH protocol which affects the overall efficiency of the enzyme.

In general, PDA-based surface modifications outperform NaOH-EDC/NHS treatment in terms of enzyme binding efficiency, catalytic effectiveness, and product generation rates, although the latter may still be beneficial in some applications. Therefore, PDA treatments are often more favorable than NaOH-EDC/NHS treatments for improving enzyme immobilization and activity.

4.5 In-depth Comparative Analysis: Different materials and designs

Polypropylene (PP), Polylactic Acid (PLA), and SLA Resin are commonly utilized materials that possess unique characteristics and are applied in specific ways. PP is renowned for its exceptional chemical resistance and mechanical robustness, while it has restrictions in terms of hydrophobicity and biocompatibility [38]. On the contrary, PLA is both biodegradable and bio-based, which makes it well-suited for environmentally conscious uses [45]. However, it does have worse mechanical qualities when compared to PP [8]. SLA Resin is utilized in high-resolution 3D printing, providing accuracy but with inherent fragility and restricted heat resistance [42,46,51].

The surface properties of these materials are dramatically changed through surface modifications, specifically by using Polydopamine (PDA) and Sodium Hydroxide-Ethyl Dimethylaminopropyl Carbodiimide/N-Hydroxysuccinimide (NaOH-EDC/NHS) treatments. PDA coatings are recognized for their ability to improve adhesion, hydrophilicity, and biocompatibility on various materials, hence increasing their suitability for advanced applications including biomedical devices and microreactors [45]. The NaOH-EDC/NHS treatment is utilized to enhance the hydrophilicity of the surface and activate it for further functionalization.

Table 7. Comparative biochemical characteristic analysis of the different designs of microreactors. A) FDM-PLA microreactor of 0.75 mm i.d. channel and FDM-PLA mixing microreactor, B)FDM-PP microreactor of 0.75 mm i.d. channel and FDM-PP mixing microreactor, C)SLA-Resin microreactor of 0.75 mm i.d. channel and SLA-Resin microreactor of 0.5 mm i.d. Channel. PDA: polydopamine, PEI: polyethylenimine, GA: glutaraldehyde, E: enzyme

A					
3D Printing Technique	**CASE**	**Immobilization yield (%)**	**Immobilized enzyme activity (U/mg)**	**Activty Yield (%)**	**STY (g/L*h)**
FDM - PLA (0,75mm)	PDA/PEI-GA-E	60.09	0.341	27.89	0.99
FDM - PLA (mixer)	PDA/PEI-GA-E	66.03	0.297	77.74	0.863
B					
3D Printing Technique	**CASE**	**Immobilization yield (%)**	**Immobilized enzyme activity (U/mg)**	**Activty Yield (%)**	**STY (g/L*h)**
FDM - PP (0,75mm)	PDA/PEI-GA-E	59.22	0.276	20.06	0.802
FDM - PP (mixer)	PDA/PEI-GA-E	60.52	0.255	72.31	0.731
C					
3D Printing Technique	**CASE**	**Immobilization yield (%)**	**Immobilized enzyme activity (U/mg)**	**Activty Yield (%)**	**STY (g/L*h)**
SLA - RESIN (0,75mm)	PDA/PEI-GA-E	54.63	0.161	13.7	0.468
SLA - RESIN (0,5mm)	PDA/PEI-GA-E	55.77	0.324	5.78	0.427

Comparative analyses of various materials have shown that PLA coated with PDA is typically the most suitable and efficient for utilization in biological settings [45]. Polypropylene exhibited high compatibility, whilst materials generated using stereolithography (SLA) had lower effectiveness. These findings highlight the significance of choosing appropriate materials and applying surface treatments to achieve favorable outcomes in microfluidic applications.

Analyzing the effectiveness of different designs we came to an outcome relatively expected. Table 7 summarizes the effectiveness of single flow microreactors with different i.d. channels and micromixers. Comparing the mixing microreactors to the simple ones, we obtained results indicating that the overall performance of the firsts was better in terms of immobilization and activity yield, fact that confirms their efficient ability for better mixing reagents and solvents as well as their capacity to immobilize bigger amount of enzyme. Nevertheless, there was a slight decrease in immobilized enzyme activity and STY which may be due to lack of stability.

At the same time the reactors with smaller internal channel diameter (0.5 mm) have better immobilization compared to the ones with bigger channels (0.75 mm) , but their efficiency in activity yield is rather lower. That might be a result of reduced enzymatic loading, but in any case their high precision and performance is remarkable. Subsequently, smaller channels achieve better contact between enzymes and substrates as it was investigated in this study, proving conclusions of previous studies [58,59].

4.6 Evaluation of Operational Stability in Microfluidic Reactors

The operational stability of the biocatalytic microreactor system was assessed by conducting 10 consecutive cycles of use, as it is demonstrated in figure 19. The oxidation of ABTS was employed as the prototype reaction, and each iteration was considered complete when the entire volume of the microreactor (12, 25, 80 μL, respectively) was processed [8]. The stability studies underscore the importance of thorough characterization in developing reliable and efficient biocatalytic systems, ensuring that enzymes can be effectively reused with minimal loss of activity.

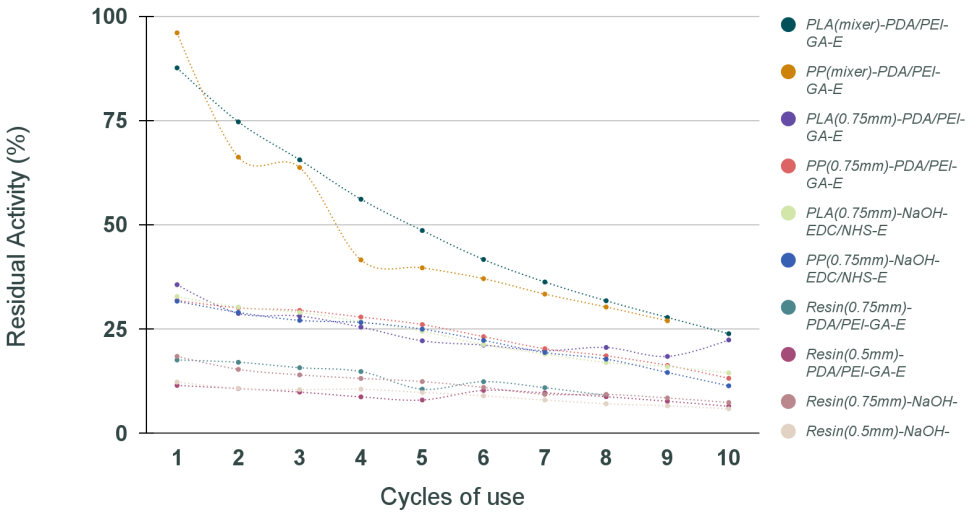

Figure 19. Operational stability of the UPO-immobilized microreactor for 10 cycles of use. 100% is representing the activity of the first cycle. Data presented as an average of three independent experiments. Standard error was ≤ 2% for all cases. Reaction Conditions: CABTS = 1mM, CH_2O_2 = 3mM, citrate buffer mM pH 4.4, T = 25oC.

The microfluidic system's operating stability is crucial, especially for industrial applications. Single flow reactors exhibit remarkable stability, as indicated by their capacity to sustain a uniform pattern of activity degradation throughout cycles. Figure 20 displays the collection of each reaction cycle in a microplate, where we can also observe the green color density that slightly decreases when it passes to the next cycle. Despite a gradual decrease in enzyme activity after each cycle, the system demonstrates excellent reusability and consistent performance. Consistency is

essential in industrial operations, since it ensures stability and reliability, which are critical for maintaining production efficiency and product quality.

a) **b)**

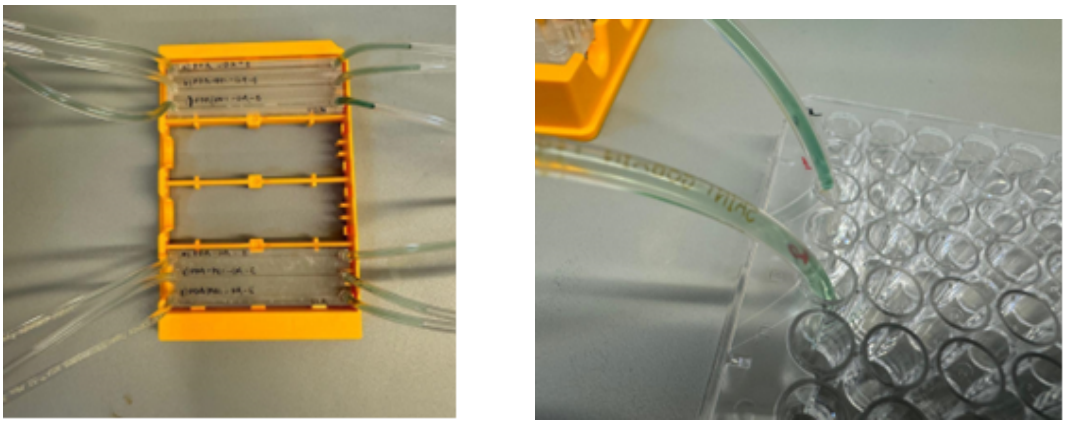

Figure 20. System of enzymatic activity measurement for the single-flow microreactor. A green color as a result of the oxidation of ABTS can be observed. The density of the color varies according to degree of the enzymatic activity. a)Tubings are connected to the microreactors inlets and outlets to facilitate the process. b)Each reaction cycle is collected in a separate well of a microplate.

On the other hand, mixing reactors display a more pronounced decline in activity, but have higher levels of initial activity. The process of collecting reaction cycles is demonstrated in Figure 21. The increased activity can be ascribed to their design, which improves the efficiency of mixing and guarantees more recent interactions between reagents. The mixing reactors are designed to enhance the reaction environment, resulting in improved reagent mixing and potentially increased activity in the initial cycles. Nevertheless, the significant decline in activity over time indicates that the system undergoes more substantial degradation or a decrease in efficiency compared to the single-flow microreactors.

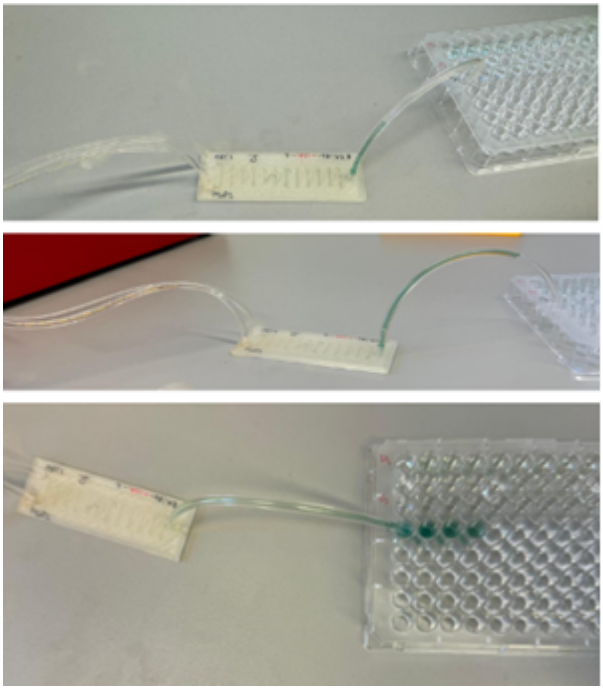

Figure 21. System of enzymatic activity measurement for the mixing microreactor. Progressive observation of each reaction cycle and product collection in microplate.

The contrast between single flow and mixing reactors emphasizes distinct advantages and compromises. Single flow reactors provide superior stability and consistent performance, rendering them more appropriate for applications that require long-term reliability and reusability. Due to their consistent drop in activity, they are well-suited for procedures that prioritize operational stability.

Conversely, mixing reactors, with their improved mixing capabilities, provide higher levels of activity at the beginning but experience more significant decreases in performance over time. Although these reactors may lack the stability of single flow reactors, they are specifically engineered to optimize performance by enhancing reagent mixing and reaction efficiency. The elevated initial activity levels suggest their capacity for use in tasks that demand improved performance, even if it compromises some stability.

To summarize, although miniature reactors may not be suitable for directly large-scale industrial applications, they offer useful insights for optimizing reactor procedures [5,7]. Single flow reactors demonstrate exceptional stability and reusability, rendering them well-suited for operations that require consistent performance over extended periods.. Mixing reactors exhibit greater reductions in performance, but they possess superior beginning activity as a result of their enhanced mixing efficiency. Comprehending these traits is essential for choosing the most suitable reactor design according to the unique demands of the application, while maintaining a balance between performance and stability as necessary.

5 CONCLUSIONS

The advancement and fine-tuning of microfluidic devices have resulted in a notable breakthrough in biocatalytic research, namely in the field of enzyme immobilization. These systems utilize the accuracy and ingenuity provided by 3D printing technology, marking a new boundary in process engineering. The incorporation of lab-on-a-chip technologies is expected to transform biocatalysis by providing accurate manipulation and immediate observation of enzyme reactions inside a compact and effective structure. By employing customized material and surface chemical methods, selective functionalization strategies seek to establish microenvironments that promote enzyme activity. These developments play a crucial role in improving microfluidic chips for efficient enzyme immobilization, therefore expanding biocatalytic applications in several academic disciplines and industrial processes.

This diploma thesis explores the design and construction of microfluidic reactors using cutting-edge 3D printing techniques in order to optimize enzymatic processes. Research and experimental work were conducted at the Institute of Technical Chemistry, Leibniz University Hannover, Germany, in the Biocatalysis and Bioprocessing research group. Multi-channel microfluidic reactors were employed to simultaneously test various assay conditions to enhance screening of UPO immobilization. The utilization of 3D printing allows for the creation of custom and consistently replicated reactors [7]. An immobilization process was devised to efficiently affix UPO onto a wide array of carrier materials, therefore expanding the functional scope and adaptability of these microreactors.

The comparative analysis for SLA Resin, FDM-PLA, and FDM-PP microreactors, demonstrated that PDA-based surface modifications, specifically those containing PEI (PDA/PEI-GA-E), outperform other treatments such as PDA-GA-E and NaOH-EDC/NHS-E. These intricate alterations improve important measurements, such as immobilization yield, enzyme activity, activity yield, and space-time yield (STY). When subjected to PDA/PEI-GA-E treatment, FDM-PLA microreactors consistently yielded superior results in enzyme activity and catalytic efficiency, rendering them well-suited for high-performance applications. The combination demonstrated improved adhesion, hydrophilicity, and overall surface functionality of PLA. PP microreactors exhibited high compatibility as well, with the PLA slightly more optimum. Although SLA-Resin microreactors were not as efficient, they experienced significant improvements through the appropriate adjustments. Nevertheless, whilst NaOH-EDC/NHS-E treatment has certain advantages for some applications and the comparative analysis affirmed certain changes on the surface, it did not yield the same degree of enhancement in biocompatibility or surface functionality as PDA, indicating its limited suitability when compared to more specialized PDA-based approaches.

The analysis of the three different microreactor designs highlights clear benefits and compromises that are essential for maximizing reactor efficiency according to individual application requirements. Results show that, single flow reactors provide long-term stability and constant performance, rendering them well-suited for extended operations, where reliability and reusability are paramount. Also, although the reactors with smaller internal diameter channels can’t handle such large volumes and have a limited capacity, they achieve more precise control and reaction efficiency, as the contact between enzyme-substrate is enhanced. Conversely, mixing reactors exhibit higher initial activity as a result of improved mixing, but also undergo a

substantial decrease in performance over time, indicating a lighter vulnerability to deterioration. Consequently, the latter reactors are more suitable for applications that prioritize initial performance rather than long-term endurance.

Overall, this work provides evidence that the PDA/PEI-GA-E treatment greatly enhances enzyme activity and catalytic efficiency in all three studied materials, proving it as a reliable and versatile technique. This treatment routinely surpasses alternative alterations, emphasizing its exceptional efficacy and dependability. However, if the primary goal is to maximize immobilization yield, it is recommended to use simpler PDA treatments such as PDA-GA-E. The PDA/PEI-GA-E treatment stands out as the most efficient and adaptable choice, delivering better performance across a range of applications. Subsequently, the technique furnishes a significant answer for many enzymatic processes, making it the most ideal choice for a universally applicable protocol.

6 OUTLOOK

Biocatalysis, a fundamental aspect of contemporary environmentally friendly chemistry, is progressively utilizing immobilized enzyme reactors (IMERs) to enhance biocatalytic systems [7]. The main problems involve enhancing manufacturing procedures, achieving a balance between extensive customization and effective reactor design, and establishing adaptable protocols for enzyme immobilization. To tackle these issues, it is necessary to streamline the implementation process across different carriers, provide scalability, and uphold the repeatability of immobilization assays. Optimizing this process can contribute to harmonize the use of small-scale implementations with large-scale industrial applications [15].

The incorporation of 3D printing technology into microfluidic systems for enzyme immobilization is poised to have a profound effect on the field of biocatalysis, providing notable progress and introducing new versatile applications. This method holds the potential to completely transform the accuracy and effectiveness of biocatalytic processes by allowing the development of extremely tailored microreactors that have improved enzyme stability and activity [23].

The combination of 3D printing and lab-on-a-chip technologies in microfluidic systems shows great potential for addressing these difficulties. Through precise manipulation of enzyme reactions in small-scale environments and introducing the ability for multiple and simultaneous reactions, these technologies enhance reaction efficiency, minimize the time and broaden the range of potential applications in both research and industry. Further exploration of specific functionalization techniques is crucial for creating microenvironments that are compatible with biomolecules. This will enable improved enzyme immobilization and stimulate innovation in biocatalytic processes.

The Fused Deposition Modeling (FDM) technique is anticipated to undergo continual evolution, which will have repercussions for many fields. Progress in material science is bolstering filament materials, such as carbon fibers and metal-infused filaments, to enhance mechanical qualities and broaden their scope of applications [43,44]. Process

optimization studies are being conducted to improve printing settings in order to maximize mechanical strength and surface polish, thus ensuring durability for a wide range of applications. Within the field of biomedical engineering, the utilization of FDM technology has already brought about significant changes in medical processes. Current research efforts are concentrated on enhancing the compatibility of devices with living tissues and refining sterilizing techniques to meet rigorous healthcare requirements.

Furthermore, the utilization of Masked Stereolithography (MSLA) technology, renowned for its exceptional precision, rapidity, and economical nature, is expected to expand significantly. The printer's capacity to generate complex and precise 3D prints makes it highly suitable for tasks like jewelry production, dentistry modeling, and prototyping.

3D printing coupled with innovative surface modification techniques are making substantial advancements in the field of biocatalytic research. The utilization of surface treatments, such as polydopamine (PDA) and polyethyleneimine (PEI), has significantly enhanced the process of enzyme immobilization and catalytic performance, particularly in the context of FDM-PLA material. Nevertheless, there are still obstacles to overcome, such as the possibility of decreased immobilization yield when using PEI, which could restrict its efficacy in applications that demand a large amount of enzymes. Moreover, SLA-resin microreactors frequently exhibit subpar enzyme performance in comparison to FDM-PLA reactors, potentially attributable to resin material-related problems. The intricacy and expense of surface treatments may pose possible challenges.

In order to overcome these problems, future research should focus on improving surface modification techniques to achieve a balance between the efficiency of immobilization and the effectiveness of enzymes. It is essential to do research on novel materials or composites that improve these features, and to integrate real-time performance monitoring with surface alterations in order to overcome existing constraints. Furthermore, the development of immobilized unspecific peroxygenase (UPO) microfluidic reactor designs that are simple to create, replicable, scalable, and cost-efficient will be highly advantageous. This involves demonstrating the use of UPO immobilization in microfluidic reactors as a versatile platform for conducting extensive biochemical experiments, with the aim of reducing process expenses and enhancing biocatalytic performance.

In summary, the combination of 3D printing with microfluidic devices for enzyme immobilization gives a significant chance for a revolutionary advancement in biocatalysis. Future success in this unique subject will be driven by ongoing breakthroughs in technology and materials, as well as focused research efforts to tackle current obstacles. These developments will enhance both research and industry applications.

7 REFERENCES

1. A. Kinner, K. Rosenthal, S. Lütz, Front. Bioeng. Biotechnol., 2021, 9, 705630. https://doi.org/10.3389/fbioe.2021.705630.
2. A. Beltrán-Nogal, I. Sánchez-Moreno, D. Méndez-Sánchez, P. Gómez de Santos, F. Hollmann, M. Alcalde, Curr. Opinion Struct.

Biol., 2022, 73, 102342. https://doi.org/10.1016/j.sbi.2022.102342.
3. L.-E. Meyer, B. Fogtmann Hauge, T. Müller Kvorning, P. De Santis, S. Kara, Catal. Sci. Technol., 2022, 12, 6473-6485. https://doi.org/10.1039/D2CY00650B.
4. J. M. Bolivar, J. M. Woodley, R. Fernandez-Lafuente, Chem. Soc. Rev., 2022, 51, 5356-5375. https://doi.org/10.1039/D2CS00083K.
5. V. Sans, Curr. Opinion Green Sust. Chem., 2020, 25, 100367. https://doi.org/10.1016/j.cogsc.2020.100367.
6. E. Gkantzou, M. Weinhart, S. Kara, RSC Sustain., 2023, 1, 1672-1685. https://doi.org/10.1039/D3SU00155E.
7. E. Gkantzou, T. Koulopoulou, H. Brass, D. Schonauer, A. Glieder, S. Kara, Catal Sci. Technol., 2024, https://doi.org/10.1039/D4CY00869C.
8. M. G. Bellou, E. Gkantzou, A. Skonta, D. Moschovas, K. Spyrou, A. Avgeropoulos, D. Gournis, H. Stamatis, Micromachines, 2022, 13, 1954. https://doi.org/10.3390/mi13111954.
9. R. A. Sheldon, ChemSusChem, 2022, 15, 202102628. https://doi.org/10.1002/cssc.202102628.
10. P. De Santis, L.-E. Meyer, S. Kara, React. Chem. Eng., 2020, 5, 1206-1220. https://doi.org/10.1039/D0RE00335B.
11. E. Gkantzou, A. Skonta, A. Tsakni, A. Polydera, D. Moschovas, K. Spyrou, A. Avgeropoulos, D. Gournis, H. Stamatis, J. Biotechnol., 2022, 350, 58-69. https://doi.org/10.1016/j.jbiotec.2022.04.005.
12. Z. Rashidi, A. Homaei, R. Fernandez-Lafuente, Process Biochem., 2024. https://doi.org/10.1016/j.procbio.2024.07.014.
13. H.-C. Yang, J.-K. Pi, K.-J. Liao, H. Huang, Q.-Y. Wu, X.-J. Huang, Z.-K. Xu, ACS Appl. Mater. Interfaces, 2014, 6, 12566-12572. https://doi.org/10.1021/am502490j.
14. M.-Y. Tsai, M.-C. Chang, H.-W. Chien, Langmuir, 2023, 39, 1234-1245. https://doi.org/10.1021/acs.langmuir.3c00526.
15. J. Chapman, A. Ismail, C. Dinu, Catalysts, 2018, 8, 238. https://doi.org/10.3390/catal8060238.
16. M. Zucca, E. Sanjust, Molecules, 2014, 19, 14139-14194. https://doi.org/10.3390/molecules190914139.
17. L. Tamborini, P. Fernandes, F. Paradisi, F. Molinari, Trends Biotechnol., 2018, 36, 878-888. https://doi.org/10.1016/j.tibtech.2017.09.005.
18. R. A. Sheldon, "The E factor 25 years on: the rise of green chemistry and sustainability," Green Chem., 2016, 19, 18-43. https://doi.org/10.1039/C6GC02157C.
19. B. Reus, M. Damian, F. G. Mutti, J. Catal. Res., 2024. https://doi.org/10.1007/s41981-024-00315-2.
20. C. W.iles, P. Watts, Green Chem., 2012, 14, 38-54. https://doi.org/10.1039/C1GC16022B
21. L.-E. Meyer, M. Hobisch, S.Kara, Curr. Op. in Biotech., 2022, 78, 102835. https://doi.org/10.1016/j.copbio.2022.102835
22. C. J.-G., P. Poechlauer, Q. B. Broxterman, B.S. Yang, D. am Ende, J. Baird., C. Bertsch, R. E. Hannah, P. Dell'Orco, H. Noorman, S. Yee, R. Reintjens, A. Wells, V. Massonneau, J. Mandley, Org. Process Ress. Dev., 2011, 15, 4, 900-911. https://doi.org/10.1021/op100327d
23. Dr. M. Michaud, Dr. G. Noglaton, Dr. Z. Anxionnaz-Minvielle, ChemBioChem, 2024, 25. https://doi.org/10.1002/cbic.202400086
24. D. T. Monterrey, A. Menés-Rubio, M. Keser, D. Gonzalez-Perez, M. Alcalde, Curr. Opinion Green Sust. Chem., 2023, 41, 100786. https://doi.org/10.1016/j.cogsc.2023.100786.

25. M. Hofrichter, Appl. Microbiol. Biotechnol., 2010, 87, 921-929. https://doi.org/10.1007/s00253-010-2633-0.
26. A. Santos, B. R. L. Galmés, L. R. Rodrigues, ACS Catal., 2020, 10, 8460-8480. https://doi.org/10.1021/acscatal.0c03029.
27. R. Ullrich, J. Nuske, K. Schneibner, J. Spantzel, M. Hofrichter, Mycology, 2004, 70, https://doi.org/10.1128/AEM.70.8.4575-4581.2004.
28. M. Hobisch, D. Holtmann, P. Gomez de Santos, M. Alcalde, F. Hollmann, S. Kara, Biotechnol. Adv., 2021, 51, 107615. https://doi.org/10.1016/j.biotechadv.2020.107615.
29. M. Hofrichter, H. Kellner, M. J. Pecyna, R. Ullrich, Adv. Exp. Med. Biol., 2015, 851, 135-161. https://doi.org/10.1007/978-3-319-16009-2_13.
30. S. N. Charlton, M. A. Hayes, ChemMedChem, 2022, 17, 1155-1163. https://doi.org/10.1002/cmdc.202200115.
31. R. K. Zhang, X. Huang, F. H. Arnold, Curr. Opinion Chem. Biol., 2019, 49, 67-75. https://doi.org/10.1016/j.cbpa.2018.10.004.
32. R. Ullrich, M. Hofrichter, Appl. Microbiol. Biotechnol., 2007, 77, 745-752. https://doi.org/10.1007/s00253-007-0942-8.
33. A. A. Maldonado, J. Guo, W. Niu, J. of Biot., 2024, 385, 1-12. https://doi.org/10.1016/j.jbiotec.2024.02.013.
34. M. Zucca, E. Sanjust, Molecules, 2014, 19, 14139-14194. https://doi.org/10.3390/molecules190914139.
35. J. M. Woodley, React. Chem. Eng., 2024, 8, 2024. https://doi.org/10.1039/D3RE00703K.
36. I. Gibson, D. W. Rosen, B. Stucker, *Additive Manufacturing Technologies: 3D Printing, Rapid Prototyping, and Direct Digital Manufacturing*, Springer, 2015. https://doi.org/10.1007/978-1-4939-2113-3.
37. E. Sanchez-Rexach, T. G. Johnston, C. Jehanno, H. Sardom, A. Nelson, Chem. Mater., 2020, 32, 8874-8892. https://doi.org/10.1021/acs.chemmater.0c02008.
38. O. S. Carneiro, A. F. Silva, R. Gomes, Mater. Des., 2015, 83, 768-776. https://doi.org/10.1016/j.matdes.2015.06.053.
39. 3D Hubs, "Introduction to FDM 3D Printing," Available at: https://www.hubs.com/knowledge-base/what-is-fdm-3d-printing/.
40. S. Waheed, J. M. Cabor, N. P. Macdonald, T. Lewis, R. M. Guijt, B. Paull, M. C. Breadmore, Lab Chip, 2016, 16, 1993-2013. https://doi.org/10.1039/C6LC00284F.
41. Y. Wang, W.-D. Muller, A. Rumjahn, A. Schwitalla, Mater., 2020, 13, 466. https://doi.org/10.3390/ma13020466.
42. A. Amini, R. M. Guijt, T. Themelis, J. De Vos, S. Eeltink, J. Chromatogr. A, 2023, 1692, 463842. https://doi.org/10.1016/j.chroma.2023.463842.
43. R.S.K.V.Ganga, R.Inala, C. S. Jowdula, P. Matti, B. N. Malleswararao, Eng. Proc., 2024, 66(1), 5, https://doi.org/10.3390/engproc2024066005.
44. A. Kantaros, E. Soulis, F. I. T. Petrescu, T. Ganetsos, 2023, 16(8), 6210, https://doi.org/10.3390/ma16186210.
45. E. H. Baran, H. Y. Erbil, Colloids Interfaces, 2019, 3, 43. https://doi.org/10.3390/colloids3020043.
46. N. P. Macdonald, J. M. Carbot, P. Smejkal, R. M. Guijt, B. Paull, M. C. Breadmore, Anal. Chem., 2017, 89, 3816-3826. https://doi.org/10.1021/acs.analchem.7b00136.
47. J. Frizzo, Tech. Rom. J. of App. Sc. and Tech., 2020, 2(7), 1-7,

https://doi.org/10.47577/technium.v2i7.1520.
48. E.R.Zhiganshina, M.V. Arsenyev, S. A. Chesnokov, Pol. Sc. Series B, 2023, 65, 247-269. https://doi.org/10.1134/S1560090423700999
49. J. Prusa, M. Bach, *Basics of 3D Printing* [PDF], SlideShare, 2019. Available at: https://de.slideshare.net/slideshow/basicsof3dprintingpdf/255908727.
50. P. Ozog, H. Elsayed, L. Grigolato, G. Savio, J. Kraxner, D. Galusek, E. Bernardo, J. of the Eur. Ceram. Soc., 2022, 42, 6192-6198. https://doi.org/10.1016/j.jeurceramsoc.2022.06.057.
51. "SLA Resin 3D Printing Guide," Available at: https://all3dp.com/1/sla-resin-3d-printing-guide/.
52. F. P. W. Melchels, J. Feijen, D. W. Grijpma, Biomaterials, 2010, 31, https://doi.org/10.1016/j.biomaterials.2010.04.050.
53. A. Davoudinejad, Add. Manuf., 2021, 159-181. https://doi.org/10.1016/B978-0-12-818411-0.00007-0.
54. "Desktop Millifluidics with SLA 3D Printing," Formlabs White Paper, Available at: https://3d.formlabs.com/white-paper-desktop-millifluidics-with-sla-3dprinting/#form.
55. I. D. Savu, S. V. Savu, D. Simion, N.-A. Sîrbu, M. Ciornei, S. A. Rațiu, "Study on the Influence of Process Parameters on the Dimensional Accuracy of FDM 3D Printed Parts," Mater. Plast., 2019, 56, 683-688. https://revmaterialeplastice.ro/pdf/35%20SAVU%204%2019.pdf.
56. Dr. M. M. C. H. van Scie, Dr. A. T. Kaczmarek, Dr. F. Tieves, P. G. de Santos, Dr. C. E. Paul, Prof. I. W. C. E. Arends, Prof. M. Alcalde, Prof. G. Schwarz, Prof. F. Hollmann, ChemCatChem, 2020, 12, 3186-3189. https://doi.org/10.1002/cctc.201902297.
57. H. B. Musgrove, M. A. Catterton, R. R. Pompano, Anal. Chim. Acta, 2022, 1209. https://doi.org/10.1016/j.aca.2022.339842.
58. K. Awawdeh, M. A. Buttkewitz, J. Bahnemann, et al., Microsyst. Nanoeng., 2024, 10, 100. https://doi.org/10.1038/s41378-024-00738-w.
59. A. Enders, I. G. Siller, K. Urmann, M. R. Hoffmann, J. Bahnemann, Small, 2018, 15, 9. https://doi.org/10.1002/smll.201804326.
60. S. Hossain, I. Lee, S. M. Kim, K.-Y. Kim, Chem. Eng. J., 2017, 327, 268-277. https://doi.org/10.1016/j.cej.2017.06.106.
61. M. Schneider, N. Fritzsche, A. Puciul-Malinowska, A. Baliś, A. Mostafa, I. Bald, S. Zapotoczny, A. Taubert, Polymers, 2020, 12(8), 1711. https://doi.org/10.3390/polym12081711.
62. C.-G. Li, Q. Yang, D. Chen, H. Zhu, J. Chen, R. Liu, Q. Dang, X. Wang, RSC Adv., 2022, 12, 30423-30435. https://doi.org/10.1039/D2RA05130C.
63. Y. Lv, H. C. Yang, H. Q. Liang, Z. K. Xu, J. Membr. Sci., 2014, 476, 50-58. https://doi.org/10.1016/j.memsci.2014.11.024.
64. K. T.sriwong and T. Matsuda, React. Chem. & Eng., 2022, 7, 1053-1060. https://doi.org/10.1039/D2RE00040G
65. R. A. Sheldon, J. M. Woodley, Chem. Rev., 2018, 118, 801-838. https://doi.org/10.1021/acs.chemrev.7b00203.
66. H. Zhang, J. Luo, S. Li, Y. Wei, Y. Wan, Langmuir, 2018, 34, 1297-1306. https://doi.org/10.1021/acs.langmuir.7b02860.
67. O. Barbosa, C. Ortiz, A. Berenguer-Murcia, R. Torres, R. C. R.odrigues, R. Fernandez-Lafuente, RSC Adv., 2014, 4, 1583-1600. https://doi.org/10.1039/C3RA45991H.
68. R. C. Rodrigues, C. Ortiz, A. Berenguer-Murcia, R. Torres, R.

Fernandez-Lafuente, Chem. Soc. Rev., 2013, 42, 6290-6307. https://doi.org/10.1039/C2CS35231A.
69. M. Yan, X. An, S. Duan, Z. Jiang, X. Liu, X. Zhao, Y. Li, Carbohydr. Polym., 2022, 296, 119983. https://doi.org/10.1016/j.carbpol.2022.119983.
70. D.-H. Zhang, L.-X. Yuwen, L.-J. Peng, Int. J. Electrochem., 2013, 2013, 946248. https://doi.org/10.1155/2013/946248.
71. B. S. Wolfenden, R. L. Willson, J. Chem. Soc., Perkin Trans. 2, 1982, 805-812. https://doi.org/10.1039/P29820000805.
72. P. K. Smith, R. I. Krohn, G. T. Hermanson, A. K. Mallia, F. H. Gartner, M. D. Provenzano, E. K. Fujimoto, N. M. Goeke, B. J. Olson, D. C. Klenk, Anal. Biochem., 1985, 150, 76-85. https://doi.org/10.1016/0003-2697(85)90442-7.
73. R. A. Sheldon, S. van Pelt, Chem. Soc. Rev., 2013, 42, 6223-6235. https://doi.org/10.1039/C3CS60075K.
74. R. A. Sheldon, Adv. Synth. Catal., 2007, 349, 1545-1559. https://doi.org/10.1002/adsc.200700150.
75. "Post-Processing and Finishing SLA Prints," Formlabs, Available at: https://formlabs.com/eu/blog/post-processing-and-finishing-sla-prints/.
76. J. Stouten, G. H. M. Schnelting, J. Hul, N. Sijstermans, T. Darikwa, C. Ye, K. Loos, V. S. D. Voet, K. V. Bernaerts, ACS Appl. Mater. Interfaces, 2023, 15, 27110-27119. https://doi.org/10.1021/acsami.3c01669.
77. L. Dal Magro, J. F. Kornecki, M. P. Klein, R. C. Rodrigues, Enzyme Microb. Technol., 2020, 132, 109397. https://doi.org/10.1016/j.enzmictec.2019.109397.
78. E. Gkantzou, J. Biotechnol., 2022, 350, 58-69. https://doi.org/10.1016/j.jbiotec.2022.04.005.
79. A. V. Chatzikonstantinou, E. Gkantzou, D. Gournis, M. Patila, H. Stamatis, Adv. Colloid Interface Sci., 2018, 257, 55-65. https://doi.org/10.1016/j.cis.2018.04.003.
80. M. J. E. Fischer, Methods Mol. Biol., 2010, 627, 55-72. https://doi.org/10.1007/978-1-60761-670-2_3.